International Journal of Nanomedicine

Dovepress
open access to scientific and medical research

Open Access Full Text Article

REVIEW

Targeted Drug Delivery Systems for Curcumin in Breast Cancer Therapy

Mian Huang[1], Bing-Tao Zhai[1,2], Yu Fan[3], Jing Sun[1], Ya-Jun Shi[1], Xiao-Fei Zhang[1], Jun-Bo Zou[1], Jia-Wen Wang[1], Dong-Yan Guo[1,4]

[1]School of Pharmacy, Shaanxi University of Chinese Medicine, Xi'an, 712046, People's Republic of China; [2]State Key Laboratory of Research & Development of Characteristic Qin Medicine Resources (Cultivation), Shaanxi University of Chinese Medicine, Xi'an, 712046, People's Republic of China; [3]School of Basic Medicine, Shaanxi University of Chinese Medicine, Xi'an, 712046, People's Republic of China; [4]Shaanxi Key Laboratory of Chinese Medicine Fundamentals and New Drugs Research, Shaanxi University of Chinese Medicine, Xi'an, 712046, People's Republic of China

Correspondence: Dong-Yan Guo, Email 2051080@sntcm.edu.cn

Abstract: Breast cancer (BC) is the most prevalent type of cancer in the world and the main reason women die from cancer. Due to the significant side effects of conventional treatments such as chemotherapy and radiotherapy, the search for supplemental and alternative natural drugs with lower toxicity and side effects is of interest to researchers. Curcumin (CUR) is a natural polyphenol extracted from turmeric. Numerous studies have demonstrated that CUR is an effective anticancer drug that works by modifying different intracellular signaling pathways. CUR's therapeutic utility is severely constrained by its short half-life in vivo, low water solubility, poor stability, quick metabolism, low oral bioavailability, and potential for gastrointestinal discomfort with high oral doses. One of the most practical solutions to the aforementioned issues is the development of targeted drug delivery systems (TDDSs) based on nanomaterials. To improve drug targeting and efficacy and to serve as a reference for the development and use of CUR TDDSs in the clinical setting, this review describes the physicochemical properties and bioavailability of CUR and its mechanism of action on BC, with emphasis on recent studies on TDDSs for BC in combination with CUR, including passive TDDSs, active TDDSs and physicochemical TDDSs.

Keywords: breast cancer, curcumin, targeted drug delivery system, passive targeting, active targeting, physicochemical targeting

Introduction

The most prevalent type of cancer and the main reason for cancer-related deaths in women globally is breast cancer (BC).[1] In 2008, approximately 1.38 million people were diagnosed with BC, with approximately 50% of patients and 60% of deaths in developing countries. Global BC survival rates vary widely, with 5-year survival rates estimated at 80% in developed countries and less than 40% in developing countries.[2] BC can be divided into four categories according to molecular subtyping: luminal A BC, luminal B BC, human epidermal growth factor receptor 2 (HER2)-positive BC and triple-negative breast cancer (TNBC).[3] Molecular subtypes are mainly based on genes expressed by cancer cells that can control the way cells behave. Common BC cell lines that express different genes are shown in Table 1,[4,5] and understanding molecular subtypes can help determine the best treatment. Luminal A BCs that are estrogen receptor (ER) positive and progesterone receptor (PR) positive but HER2 negative usually have a better prognosis and can be treated with endocrine therapy alone, with chemotherapy as an option. Luminal B BCs that are ER positive, PR negative and HER2 positive tend to grow faster than luminal A BCs, have a slightly worse prognosis and require chemotherapy combined with endocrine therapy. HER2-positive BCs that are ER and PR negative and HER2 positive tend to grow faster and have a worse prognosis than luminal BC but can often be successfully treated with targeted therapeutic agents that target the HER2 protein. Finally, TNBC, which is negative for ER, PR and HER2, has the worst prognosis of the four molecular types and is usually aggressive, unresponsive to endocrine therapy and targeted therapy, and effectively treated only by chemotherapy.[6,7] However, conventional treatment options such as chemotherapy and radiotherapy are often accompanied by serious side effects and toxicity that can

Received: 17 March 2023
Accepted: 19 June 2023
Published: 28 July 2023

Table 1 BC Cell Lines with Different Gene Expression

BC Cell Line	Sources of Species	Subtype	ER	PR	HER2	Ref., Year
MCF-7	Human	Luminal A	+	+	-	2010[4], 2017[5]
MCF-10A	Human	Luminal A	+	+	-	
BT-47D	Human	Luminal A	+	+	-	
BT-474	Human	Luminal B	-	+	+	
SKBR3	Human	HER2+	-	-	**+**	
MDA-MB-231	Human	Triple negative	-	-	-	
MDA-MB-468	Human	Triple negative	-	-	-	
Hs578T	Human	Triple negative	-	-	-	
EMT6	Mice	/	/	/	/	
4T1	Mice	/	/	/	/	
JC	Mice	/	/	/	/	

seriously affect the daily life of patients. Moreover, some studies have found that with prolonged treatment, cancer cells are able to develop resistance to chemotherapy and radiotherapy.[8] Therefore, it is particularly important to find new alternative therapies. For many years, natural drugs have received much attention from scientists for their low toxicity and side effects, and in the United States, approximately 50–60% of cancer patients use natural drugs as a complement and alternative to conventional drugs, regardless of whether they use conventional chemotherapy or radiation therapy.[9] CUR, resveratrol, lycopene, and camptothecin are some of the substances that have demonstrated modest anticancer action with few side effects.[10–13] Among them, CUR is of great interest due to its widely reported anticancer activity.

CUR (1,7-bis (4-hydroxy-3-methoxyphenyl)-1,6-heptadiene-3,5-dione) is a naturally occurring polyphenol that is obtained from the ginger family member turmeric.[14] The therapeutic effects of CUR on the nervous, respiratory, cardiovascular, urinary, reproductive, digestive and hepatobiliary, musculoskeletal and endocrine systems, as well as the skin, have been confirmed by previous studies. CUR has also been shown to be a potent anti-inflammatory, antitumor, and antioxidant agent.[15,16] However, the clinical usage of CUR is severely constrained because of its short half-life in vivo, poor stability, quick metabolism, low oral bioavailability, and 89% excretion of the medication in its original form after large oral dosages.[17,18]

One of the most practical approaches to resolving the aforementioned problems is the development of targeted medication delivery systems based on nanomaterials.[19] Nanotargeted drug delivery systems have emerged as viable chemotherapeutic drug delivery techniques during the past few decades thanks to their major contributions to cancer diagnostics and treatment.[20] By extending the circulation time of insoluble medications and improving their accumulation in tumor tissues through increased permeability and retention effects (EPR), nanotargeted drug delivery systems can successfully improve the solubility and in vivo drug distribution of insoluble pharmaceuticals.[21–23] Despite their high levels in tumor tissues, however, they do not promote efficient drug uptake by tumor cells. To actively target tumor cells, particular ligands or antibodies can be used to modify the surface of nanoparticles. This can help to increase the selectivity of medications for tumor cells, lessen their distribution in nontarget tissues, and lessen their side effects. Because tumor tissues and cells have different structural and physicochemical properties than normal tissues and cells, endogenous tumor microenvironment-responsive drug delivery systems can be designed, and exogenous stimulation-responsive drug delivery systems can be designed using the unique properties of the carriers themselves, such as pH, light, temperature, and magnetism, to address the issue of in vivo local drug release.[24–26]

The design and development of various CUR-TDDSs, including passive and active TDDSs and physicochemical TDDSs, are the focus of this review, with a concentration on their therapeutic efficacy in BC. The main characteristics of CUR and the pharmacokinetics and efficacy of CUR nanoformulations in vitro and in vivo are discussed, thus providing new ideas for future clinical applications of CUR (Figure 1).

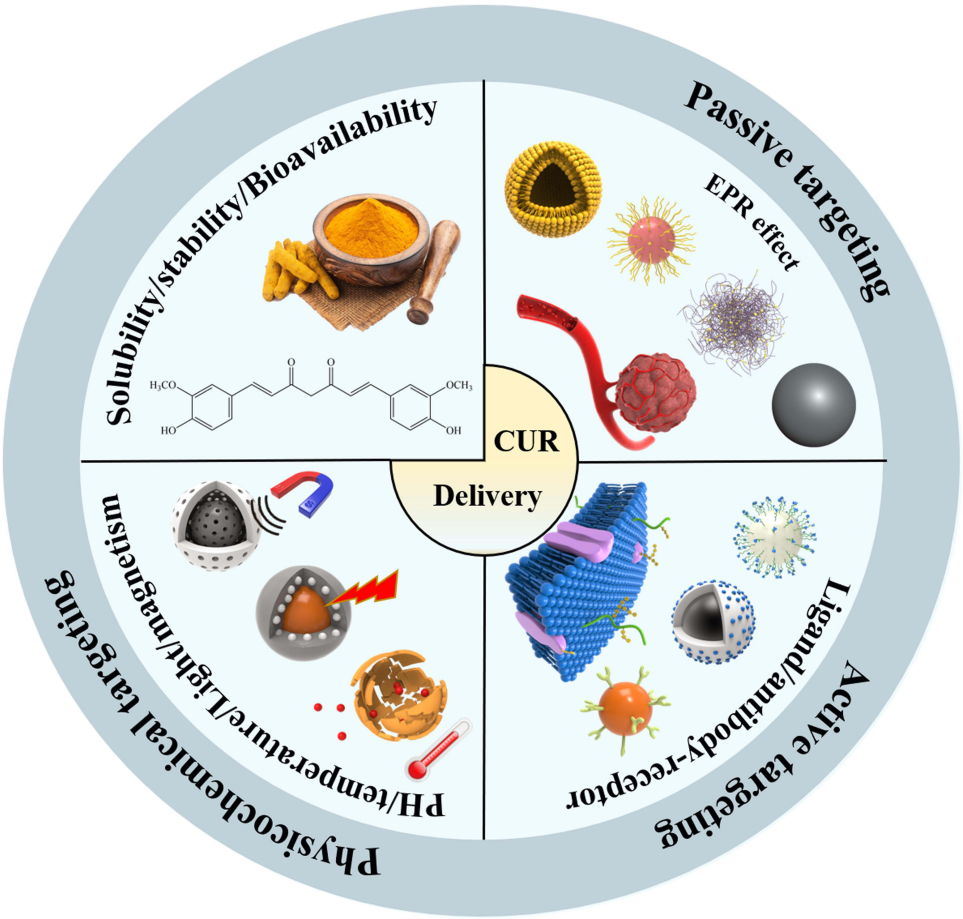

Figure 1 Schematic diagram of the physical and chemical properties of curcumin and its classification of targeted drug delivery systems.

Key Properties of Curcumin

CUR comes from the plant *Curcuma longa* L. and is a low-molecular-weight polyphenol. It is a safe and all-natural additive that has been sanctioned for use in food production by the governments of numerous nations.[27] The components extracted from turmeric contain a variety of CUR-like compounds, mainly CUR, demethoxycurcumin and bisdemethoxycurcumin.[28] Among them, CUR is the most abundant polyphenolic compound in turmeric.[29] For many years, CUR has received attention for its broad range of anticancer activities.[30,31] The following section will focus on the physicochemical properties and bioavailability of CUR and its anticancer mechanism (especially in BC).

Physicochemical Properties

CUR has the chemical formula $C_{21}H_{20}O_6$ and a relative molecular mass of 368.38.[32] It is composed of two benzene rings replaced with hydroxyl and methoxy groups and joined by a seven-carbon keto-enol junction (Figure 2A).[33] CUR has two reciprocal isomers, keto and enol (Figure 2B).[34] Under neutral and acidic pH conditions, the keto form dominates, while under basic conditions, only the enol interconversion isomer is present, which can be explained by the intramolecular hydrogen bonding of the enol form.[35] CUR is almost insoluble in neutral and acidic aqueous solutions at room temperature. CUR is highly soluble in both polar nonprotonic and polar protonic solvents, with the following order of solubility: acetone > 2-butanone > ethyl acetate > methanol > ethanol > 1,2-dichloroethane > isopropanol > ether > benzene > n-hexane. In addition, dimethyl sulfoxide is a common solvent that can dissolve CUR at concentrations up to 11 mg/mL, while the concentration in ethanol is only 1 mg/mL.[36] Under alkaline conditions (pH > 10), CUR is completely deprotonated and has a maximum absorption at 467 nm. The pKa of CUR is 8.54, and CUR has three unstable protons at neutral pH, one of which is an alkene proton and two are phenolic protons.[37] CUR is unstable under

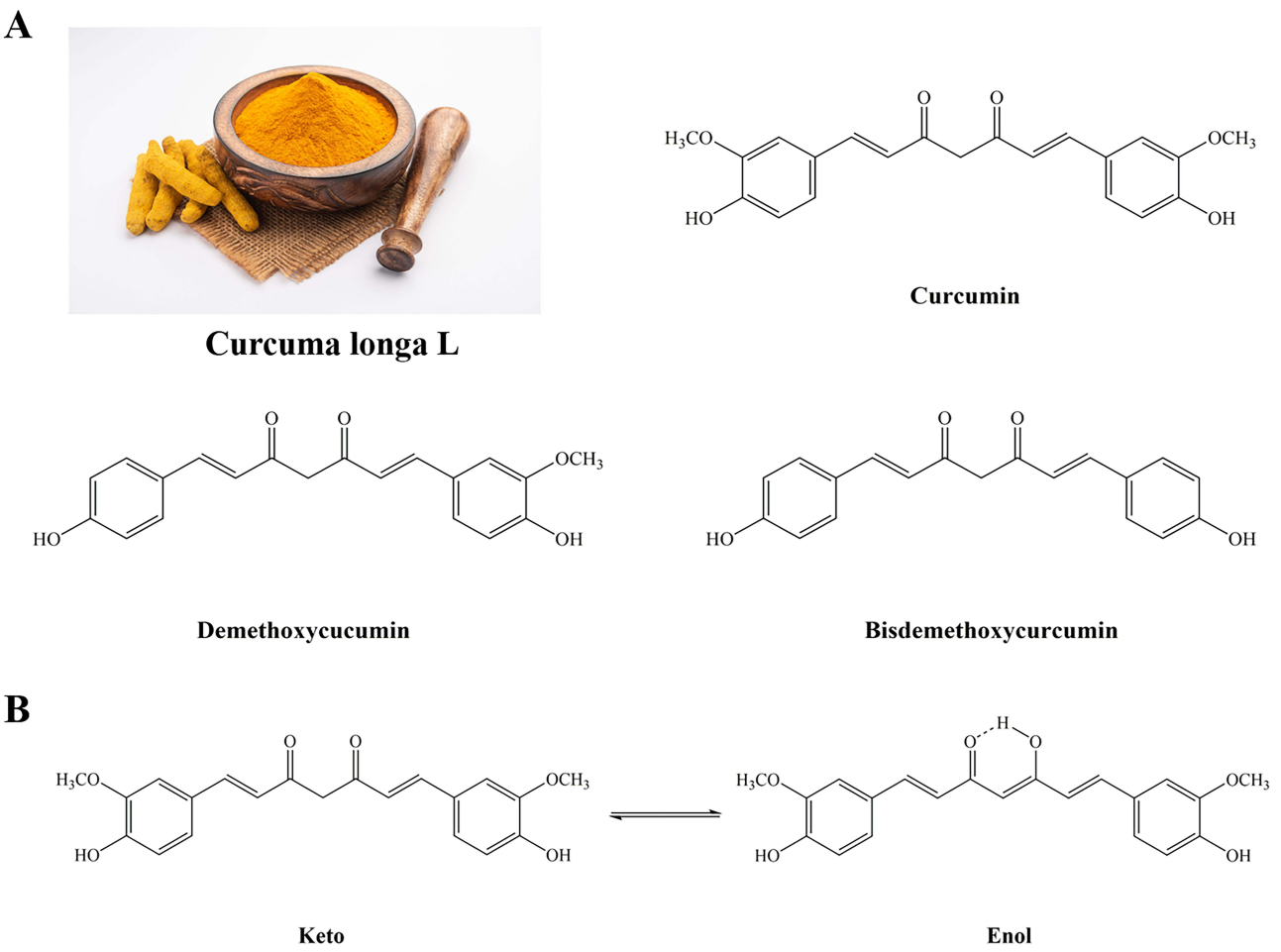

Figure 2 (**A**) Structural formulae of the three main curcumin-like compounds extracted from turmeric. (**B**) Mutual isomers of curcumin.

physiological pH conditions and is susceptible to degradation through solvolysis, photodegradation and autoxidation, with solvolysis and photodegradation being the main pathways. Solvolysis involves nucleophilic substitution or elimination of solvent molecules. The α, β-unsaturated ketone fraction of CUR is the main site of nucleophilic attack (Michael addition). In alkaline buffered aqueous solutions, solvolysis of the heptadienone chain leads to degradation of 90% of CUR, yielding products such as vanillin, ferulic acid, and ferulic aldehyde.[38,39] CUR undergoes autoxidation through a chain of free radical reactions, binding to oxygen and yielding dicyclopentadiene products.[40] It has been shown that CUR is susceptible to photodegradation both in the solid-state and in solution; therefore, CUR samples should be stored away from light. Its photochemical degradation products are mainly ferulic acid, ferulic aldehyde, vanillin and vanillic acid (Figure 3).[41]

Bioavailability

The important pharmacokinetic term bioavailability relates to the rate and degree of drug absorption into the human circulation. It is a complex process that includes absorption, distribution, metabolism and excretion of drugs.[42,43] Due to its low bioavailability, poor pharmacokinetics, and short half-life in the gastrointestinal tract, the clinical usefulness of CUR is restricted.[44,45] For example, a preclinical study in rats showed that oral administration of 500 mg/kg CUR produced peak blood concentrations of only 1.8 ng/mL.[46] Free CUR was detected in the plasma of only one subject 30 minutes after ingestion of a 10 g dose of CUR, and no free CUR was detected in plasma samples from any other subject (less than 50 ng/mL), indicating low bioavailability and high metabolism of CUR, according to a pharmacokinetic study of CUR in healthy subjects.[47,48] CUR is metabolized mainly in the liver and to a lesser extent in the intestine, and CUR

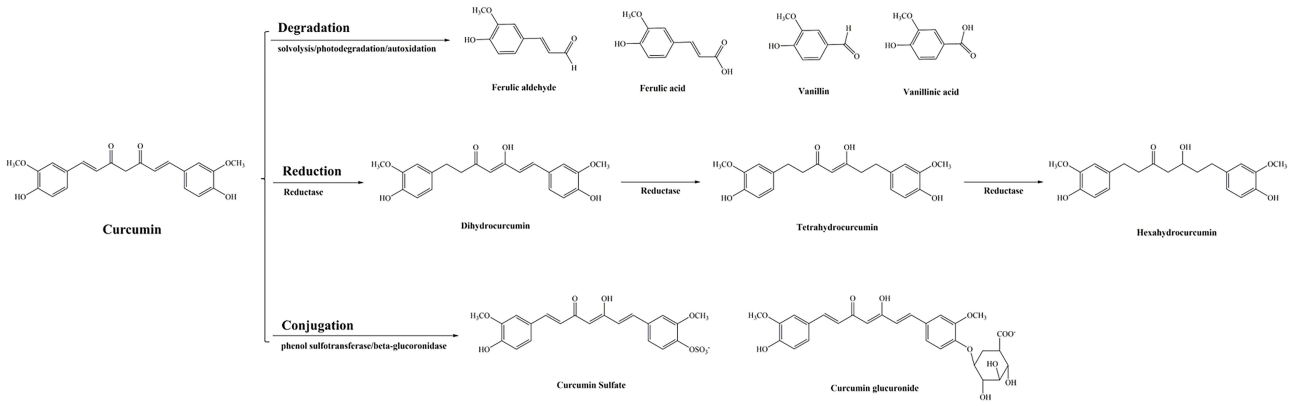

Figure 3 Curcumin degradation and metabolites.

metabolism occurs mainly by reduction and conjugation.[49–51] The reduction of CUR occurs mainly at the double bond of the CUR heptadienone chain and is mainly promoted by NADPH-dependent reductase, ethanol dehydrogenase and an unidentified microsomal enzyme to produce dihydro, tetrahydro and octahydro CUR.[40] Another major metabolic pathway of CUR in vivo is glucuronidation/sulfonation conjugation, which occurs mainly at the phenolic oxygen of CUR, also through enzymatic reactions. For example, the human phenol sulfotransferase isozymes SULT1A1 and SULT1A3 catalyze the O-sulfonation of CUR.[52] Similarly, glucuronidation is catalyzed by UDP-glucuronosyltransferase.[53]

Mechanism of Action of Curcumin in the Treatment of Breast Cancer

BC, as one of the most common malignant tumors in women, is treated with anti-estrogen therapy in approximately 70% of patients who are ER positive.[54] The use of a single molecule, however, appears to have little effect on the network of crosstalk and negative feedback loop cells in complex malignancies, according to mounting data in recent years.[55] To achieve optimal therapeutic outcomes, multitargeting of different pathological signaling pathways is considered a major trend to kill drug-resistant BC cells. Researchers are searching for effective drug candidates to better treat BC.[56] CUR is considered to be an effective anticancer agent that modulates multiple intracellular signaling pathways, especially because it is a natural chemical present in plants, offering a natural advantage over synthetic compounds in terms of safety issues.[57,58] The following section will focus on the therapeutic role of CUR in BC, including the molecular targets and mechanisms of action (Figure 4).

First, CUR induces downregulation of the EZH2 oncogene by stimulating the mitogen-activated protein kinase (MAPK) pathway of c-Jun amino-terminal kinase (JNK), extracellular regulatory protein kinase (ERK) and p38 kinase; blocking NF-κB expression; inhibiting HIF-1α and HIF-2α protein expression; promoting peroxisome proliferator-activated receptor-γ (PPAR-γ) protein expression and increasing p53 phosphorylation; inhibiting vascular endothelial growth factor (VEGF) and basic fibroblast growth factor (b-FGF) transcript levels; inhibiting the expression of ER downstream genes pS2 and TGF-β; and inhibiting the activity of epidermal growth factor receptor (EGFR) and HER-2/neu to suppress BC cell proliferation.[59–63] In addition, it has been shown that CUR inhibits cell proliferation by inducing unipolar spindle formation and cycle arrest in late G2M and S phases in BC cells.[64] Zhou et al[65] showed that the combination of CUR and mitomycin for BC treatment enhanced G1 phase block and inhibited tumor growth by regulating the expression levels of Cyclin D1, Cyclin E, Cyclin A, cyclin-dependent kinase 2 (CDK 2), cyclin-dependent kinase 4 (CDK4), p21, and p27. Second, CUR inhibits matrix metalloproteinase-2 (MMP-2) and matrix metalloproteinase-9 (MMP-9), activates matrix metalloproteinase inhibitor 1 (TIMP-1) and matrix metalloproteinase inhibitor 4 (TIMP-4) gene expression, downregulates chemokine ligand 1 (CXCL-1) and chemokine ligand 2 (CXCL-2) expression by inhibiting NF-κB and activating AP-1, antagonizes protein kinase B (PKB) expression and activates cellular autophagy to inhibit BC cell invasion and migration.[66–68] Third, CUR induces apoptosis in BC cells by promoting the expression of cleaved PARP and caspase-3, downregulating insulin-like growth factor 1 (IGF-1), promoting the expression of pro-apoptotic protein (Bax) and inhibiting the expression of anti-apoptotic protein (Bcl-2).[69,70] Moreover, CUR downregulates the expression of VEGF, angiopoietin-1 (Ang-1), angiopoietin-2 (Ang-2),

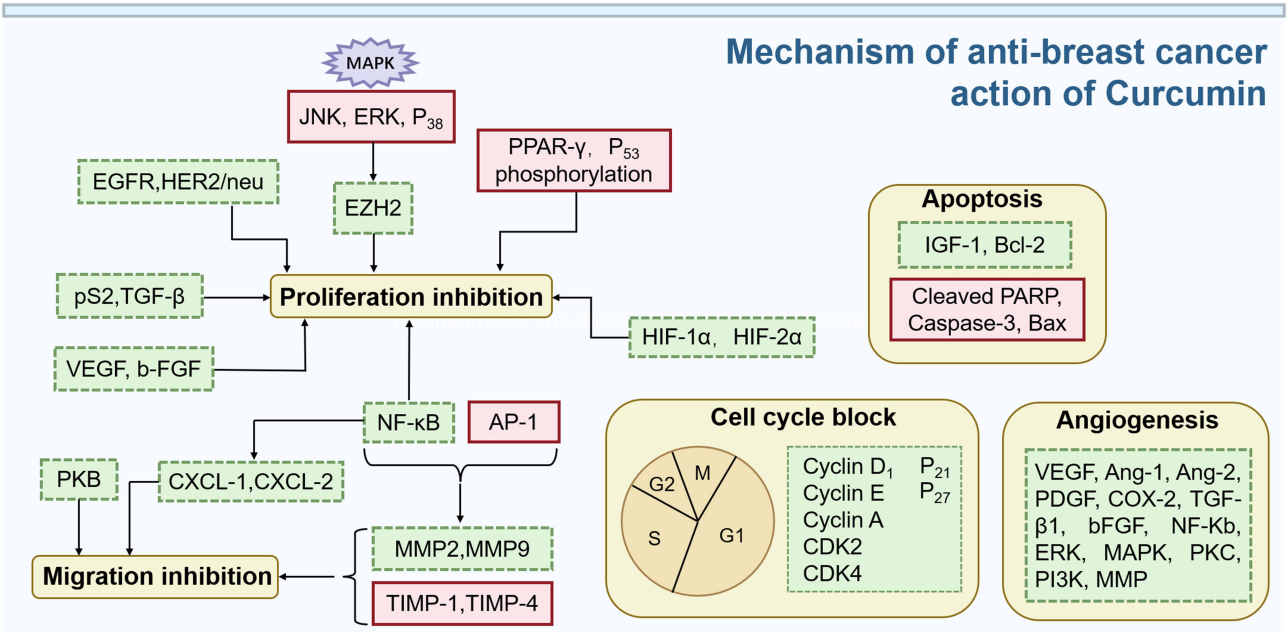

Figure 4 Mechanism of anti-breast cancer action of curcumin. Green dashed boxes indicate suppression or downward adjustment, red solid boxes indicate promotion or upward adjustment.

Abbreviations: JNK, c-Jun amino-terminal kinase; ERK, extracellular regulatory protein kinase; PPAR-γ, peroxisome proliferator-activated receptor-γ; TGF-β, transforming growth factor-β; VEGF, vascular endothelial growth factor; b-FGF, basic fibroblast growth factor; EGFR, epidermal growth factor receptor; PKB, protein kinase B; CXCL-1, chemokine ligand 1; CXCL-2, chemokine ligand 2; MMP-2, matrix metalloproteinase-2; MMP-9, matrix metalloproteinase-9; TIMP-1, matrix metalloproteinase inhibitor 1; TIMP-4, matrix metalloproteinase inhibitor 4; CDK 2, cyclin-dependent kinase 2; CDK4, cyclin-dependent kinase 4; IGF-1, insulin-like growth factor 1; Ang-1, angiopoietin-1; Ang-2, angiopoietin-2; PDGF, platelet-derived growth factor; COX-2, Cyclooxygenase-2; TGF-β1, transforming growth factor-β1; PKC, protein kinase C; PI3K, phosphoinositide 3-kinase; MMP, matrix metalloproteinase.

platelet-derived growth factor (PDGF), cyclooxygenase-2 (COX-2), transforming growth factor-β1 (TGF-β1) and basic fibroblast growth factor (bFGF) and inhibits NF-κB, extracellular-signal regulated kinases (ERK), MAPK, protein kinase C (PKC), phosphoinositide 3-kinase (PI3K), and matrix metalloproteinases to inhibit tumor angiogenesis.[71,72] Finally, some studies suggest that CUR may treat BC by modulating the immune system. It may inhibit the oncogenic effects of immunosuppressive cytokines, such as transforming growth factor beta (TGF-β) and interleukin 10 (IL-10), and reduce the loss of T lymphocytes during carcinogenesis.[73]

Curcumin Drug Delivery Systems in Breast Cancer

For years, researchers have tried to use nanodelivery systems to improve the bioavailability of CUR.[74,75] At tumor sites, the high permeability and retention of nanomaterials may improve chemotherapeutic drug accumulation.[76–79] Encapsulated systems can improve CUR solubility, bioavailability, absorption and cellular uptake by enhancing the osmotic effect and increasing the opportunity to evade renal filtration and biliary excretion.[80] Ideally, CUR nanoformulations for cancer should have stronger anticancer activity than free CUR while being nontoxic to normal cells. The effectiveness of the treatment targeting is directly correlated with patient quality of life and ultimate life expectancy. The CUR nanoagents reported in the literature for the treatment of BC can be subdivided into passive targeting, active targeting and physicochemical targeting by different targeting types. The following sections will describe the CUR drug delivery system according to different target types, focusing on its application in BC.

Passive Targeting Drug Delivery Systems

The term "passive targeting formulation" describes a method of drug delivery that relies on the anatomical and physiological distinctions between different organs and tissues to provide targeted effects.[81,82] Due to differences in microvascular structure between solid tumors and normal tissues, enhanced EPR is thought to be the passive targeting mechanism of nanocarriers to tumor sites. The microvascular endothelial gap in normal tissues is dense and structurally

intact, making it difficult for macromolecules and large particles to penetrate the vessel wall. Solid tumor tissues, on the other hand, lack lymphatic flow and have poor structural integrity, increased neovascularization, and larger gaps in the vascular wall. This difference causes large molecules or particles with a diameter of 100 nm or less to be more easily collected inside tumor tissues, which enables targeting effects (Figure 5).[83–88] Liposomes, micelles, nanogels, nanoparticles, nanoemulsions and so on can all be used as carriers in passive targeting preparations, and the main characteristics of these systems and the main points are summarized in Table 2.

Liposome-Based CUR Delivery

For several years, the biocompatibility, transport, and targeting potential of liposomes have attracted attention. A bilayer of phospholipids forms spherical vesicles known as liposomes based on the "molecular compatibility" hypothesis.[42] The treatment of drug-resistant cancers has improved as a result of recent developments in liposome formulations.[112] Hamano et al[89] designed and refined a novel liposome formulation to increase the loading capacity of CUR using automated microfluidic technology. The prepared liposomes had a particle size of 116.4 ± 5.5 nm, polymer dispersibility index (PDI) of 0.140 ± 0.025, CUR concentration of 278.7 ± 40.4 μg/mL, CUR dose recovery of 87.7 ± 10.7%, and drug loading (DL) of 17.1 ± 2.1%. In comparison to other reported liposome systems, this system had an exceptionally high loading capacity and a low PDI. Compared to the conventional CUR suspension formulation, the new formulation increased water solubility by a factor of 700 and systemic exposure by a factor of 8–20. Animal models were then used to test the anticancer activity of these liposomes and their reduced nephrotoxicity when paired with cisplatin (DDP). The outcomes demonstrated that it decreased nephrotoxicity and improved the anticancer activity of DDP in a number of animal tumor models (Figure 6). Hasan et al[90] encapsulated CUR in chitosan-coated nanoliposomes derived from three natural lecithin sources and characterized them. Finally, they investigated their growth inhibition on MCF-7 BC cells. The results showed that chitosan-coated liposomes increased their size, changed their charge from negative to positive, and obtained a higher entrapment efficiency (EE) of CUR. The growth inhibition test on MCF-7 BC cells showed that the growth inhibition increased when the liposome was coated with

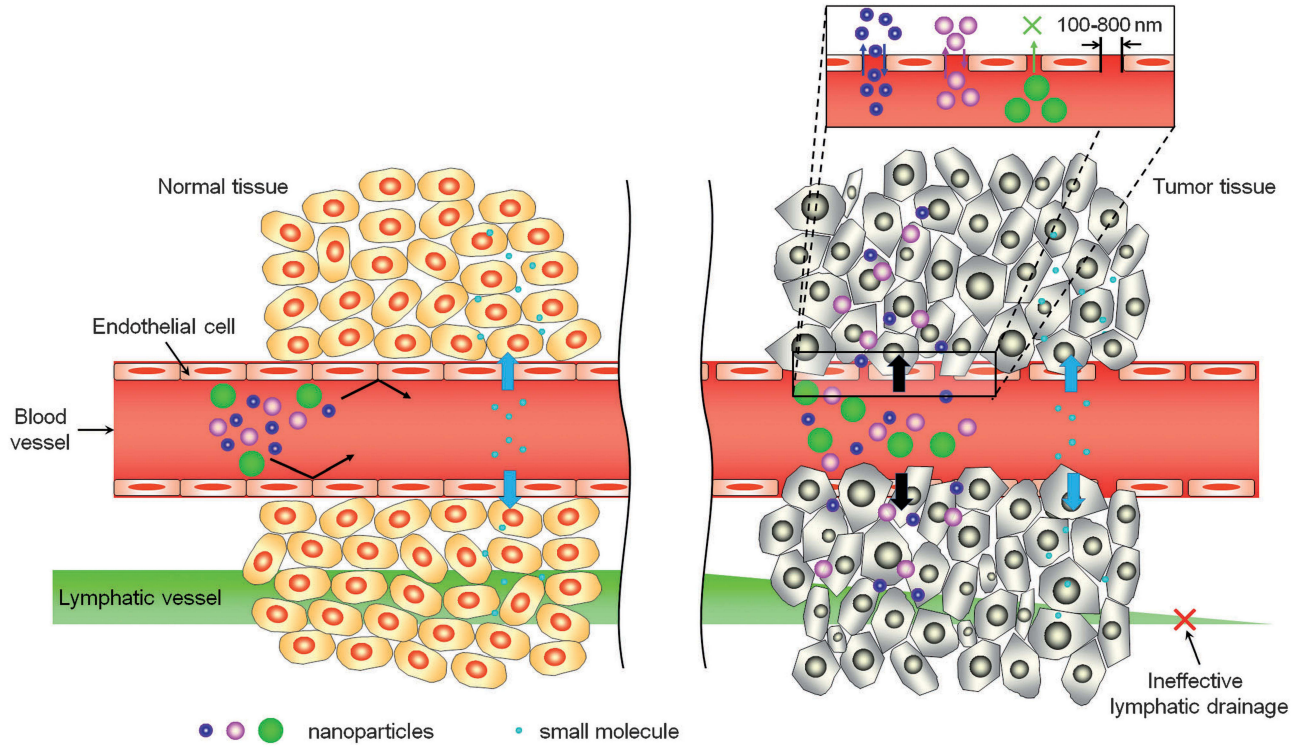

Figure 5 Transport of nanoparticles with different sizes and small molecules through normal (left) and cancerous (right) tissues. The enhanced permeability and retention (EPR) effect is a unique feature of most tumors, allowing nanoparticles of appropriate sizes to accumulate more in cancerous tissues than in normal tissues. Reproduced with permission from Sun T, Zhang YS, Pang B, et al. Engineered nanoparticles for drug delivery in cancer therapy. John Wiley and Sons.[88] © 2014 WILEY-VCH Verlag GmbH & Co. KGaA, Weinheim.

https://doi.org/10.2147/IJN.S410688 DovePress

Table 2 Passive TDDS of CUR

Drug Delivery System	Features	Characterization	Pharmacokinetics/Tissue Distribution/Efficacy	Ref., Year
CUR Liposomes	High DL	Mean Size = (116.4 ± 5.5) nm, PDI = (0.140 ± 0.025), CUR concentration = (278.7 ± 40.4) μg/mL, DL = (17.1 ± 2.1) %	Pharmacokinetic parameters: a. Liposomes/solution (20 mg/kg, *oral*.) C_{max}, AUC, BA ↑, $t_{1/2}$ ↓ b. Liposomes (20 mg/kg, *iv*.) C_{max}, AUC ↑, $t_{1/2}$ ↓; EMT6 tumor inhibition rate: DDP (15 mg/kg, *ip*.) = 46%, Liposomes (20 mg CUR/kg, *iv*.) = 39%, combination of DDP and Liposomes = 77%; B16F10 tumor inhibition rate: DDP (15 mg/kg, *ip*.) = 63%, Liposomes (20 mg CUR/kg, *iv*.) = 46%, combination of DDP and Liposomes = 74%	2019[89]
Chitosan coated liposomes (CCL)	High EE	a. Soya CCL b. Salmon CCL c. rapeseed CCL Mean Size = a: (321 ± 0.9) nm, b: (380 ± 2.8) nm, c: (327 ± 3.2) nm, PDI = a: (0.24 ± 0.01), b: (0.24 ± 0.02), c: (0.25 ± 0.02), zeta potential = a: (61.8 ± 0.6) mV, b: (65.6 ± 0.4) mV, c: (67.9 ± 0.3) mV, EE = a: 87.15%, b: 88.61%, c: 88.72%, Membrane Fluidity = a: (2.56 ± 0.10), b: (2.62 ± 0.20), c: (3.21 ± 0.1)	MCF-7 cells (CUR 12 μM or higher CUR concentration has a significant impact on cell index, Soya CCL and rapeseed CCL can significantly reduce the cell proliferation of cancer cells at the concentration of 20 μM, Salmon CCL can have a growth-inhibitory effect with a lower concentration (5 μM).)	2020[90]
Thiol derivatised chitosan coated liposomes	More sustained release	Mean Size = (406 ± 12) nm, PDI = (0.35 ± 0.03), zeta potential = (36.6 ± 0.57) mV, EE = (93.95 ± 3.94) %, DL = (7.95 ± 0.36) %	MCF-7 cells (The cell viability of liposomes group was higher than that of other groups at 24 hours, CUR was gradually released over time, and showed significant inhibition in the high CUR concentration group at 72 hours.)	2017[91]
DDP and CUR co-loaded Liposomes	Efficient	Mean Size = 100 nm, EE = DDP/CUR: 23.85/99.8%	MCF-7 cells (72 h, 32/20 mg/mL CUR-DDP-NLPs/free CUR-DDP, cell viability = 17.5%, 31.6%; cell apoptosis: 66.85%/32.2%, 11.1%/67.1% (late apoptosis/early apoptosis))	2021[92]
Micelles	1. Non-toxic and safe 2. High solubility	Mean size = 205 nm, zeta potential = −53 mV, DL = 4.5%, CMC = 0.654 mg/mL	4T1 tumor inhibition rate: Micelles (70 mg/kg, *ip*., 1, 4, 7, 9 day) = 31.25%	2019[93]
Micelles	1. Good biocompatibility 2. Efficient	Mean size = (175.8 ± 0.68) nm, PDI = (0.248 ± 0.075), zeta potential = (5.9 ± 0.78) mV, DL = (14.2 ± 0.24) %, EE= (98.6 ± 1.48) %, CMC = 20 mM	B16F10 cells viability (a. 6 h, 50 μg/mL: CUR = (58.2 ± 4.2) %, micelles = (42.8 ± 3.2) % b. 24 h, 50 μg/mL: micelles = (42.4 ± 3.5) %); MDA-MB-231 cells viability (a. 6 h, 50 μg/mL: CUR = (59.6 ± 4.2) %, micelles = (58.2 ± 4.6) % b. 24 h, 50 μg/mL: micelles = (45.2 ± 1.4) %)	2018[94]
Nanogel	Good biocompatibility	Mean size = (452 ± 8) nm, zeta potential = (−27 ± 4) mV, EE = (65 ± 2) %	MCF-7 cells (CUR showed severe toxicity to MCF-7 cells in the concentration range of 3.125 to 50 μg/mL. 50 μg/mL nanogels were acutely toxic to MCF-7 cells. At other doses, CUR-loaded nanogels were less toxic than CUR and remained toxic to cells at a dose of 12.5 μg/mL.)	2016[95]

Nanogel	1. Reduces DDP toxicity 2. Efficient	Mean size = (94.12 ± 3.85) nm, PDI = (0.39 ± 0.07), zeta potential = (5.9 ± 0.78) mV, DL= CisOH/ CUR: 22.3/4.4%, CMC= (40.97 ± 4.04) ppm	MCF-7 cells (48 h, DDP: IC_{50} = 0.61 ± 0.03 μg/ mL, HP403@CisOH: IC_{50} = (8.5 ± 0.7) μg/mL, HP403@CisOH@Cur: IC_{50} = (19.99 ± 0.89) μg/mL); MCF-7 tumor volume reduction rate on day 8: DDP (3 mg/kg, *ip*., 1, 3, 5, 7, 9, 11, 13 day) = 80%, HP403@CisOH (3 mg/kg, *ip*., 1, 3, 5, 7, 9, 11, 13 day) = 78%, HP403@CisOH@Cur (3 mg/kg, *ip*., 1, 3, 5, 7, 9, 11, 13 day) = 70%	2022[96]
CUR-SLNs	Efficient	Mean size = 40 nm, zeta potential = (−25.3 ± 1.3) mV, DL= 23.38%, EE = 72.47%	SKBR3 cells (48 h, CUR: IC_{50} = 28.42 μM, CUR-SLNs: IC_{50} = 18.78 μM; cell apoptosis: CUR = 29%, CUR-SLNs = 36.7%); SKBR3 cells (CDK4, Bcl-2 ↓, Bax ↑)	2018[97]
CUR-SLNs	1. High DL 2. Good bioavailability 3. Stability	Mean size = below 200 nm, EE = (70–75) %	MDA-MB-231 cells and JC cells (Enhancement of DOX efficacy: CUR-SLNs > CUR) JC tumor inhibition rate: CUR-CS-SLN + DOX (CUR-CS-SLN: 5 mg CUR/kg, DOX: 5 mg/kg, *iv*., 1, 7, 14 day) > CUR-SLN + DOX (CUR-SLN: 5 mg CUR/kg, DOX: 5 mg/kg, *iv*., 1, 7, 14 day) > CUR-SLN (5 mg CUR/kg, *iv*., 1, 7, 14 day) > CUR-CS-SLN (5 mg CUR/kg, *iv*., 1, 7, 14 day) > CUR + DOX (CUR: 5 mg/kg, DOX: 5 mg/kg, *iv*., 1, 7, 14 day) > CUR (5 mg/kg, *iv*., 1, 7, 14 day) > DOX (5 mg/kg, *iv*., 1, 7, 14 day)	2020[98]
CUR-loaded PLGA nanoparticles	1. High DL 2. Good biocompatibility	Mean Size = (81.05 ± 3.85) nm, PDI = 0.107, zeta potential = +31.8 mV, DL = 21.8%, EE = 69.1%	MDA-MB-231 cells (24 h, CUR: IC_{50} = 43.91 μM, nanoparticles: IC_{50} = 24.63 μM; cell apoptosis: CUR = 20.77%, nanoparticles = 39.47%)	2017[99]
MTX and CUR co-loaded PLGA nanoparticles	1. Efficient 2. Synergetic administration	Mean Size = (148.3 ± 4.07) nm, PDI = 0.17, zeta potential = (−3.41 ± 0.8) mV, DL = MTX/CUR: (15.9 ± 4.7) / (22.1 ± 2.85) %, EE = MTX/CUR: (71.32 ± 7.8) / (85.64 ± 6.3) %	SK-Br-3 cells (24 h, nanoparticles: IC_{50} = (7.2 ± 0.2) μg/ mL; 48 h, nanoparticles: IC_{50} = (5 ± 0.4) μg/mL); Tumor inhibition rate: CUR (CUR: 2.5 mg, *iv*., 16, 17, 18, 19, 20 week (once a week)) = 19%, nanoparticles (MTX/CUR: 5/2.5 mg, *iv*., 16, 17, 18, 19, 20 week (once a week)) =76%	2019[100]
CUR-loaded Chitosan nanoparticles	High DL	Mean Size = 200 nm, PDI = 0.34, zeta potential = + 26.66 mV, DL = 67%, EE = 40.2%	MCF7 cells (24 h, CUR: IC_{50} = (20.63 ± 2.2) μg/mL, nanoparticles: IC_{50} = (1.45 ± 0.24) μg/mL); MCF7 cells (NF-κb, TNF-α, IL-6, Bcl-2 ↓)	2021[101]
CUR-loaded Chitosan nanoparticles	Synergetic administration	Mean Size = (652 ± 10) nm, EE = 51.67%	4T1 cells viability (TRAIL-PMSCs + nanoparticles: 24/48/72 h: 58/41/33%); 4T1 tumor inhibition rate: TRAIL-PMSCs + nanoparticles (1×10^6 TRAIL-PMSCs + 100 μg nanoparticles in 250 μL PBS) = 44%	2018[102]

(*Continued*)

https://doi.org/10.2147/IJN.S410688

Table 2 (Continued).

Drug Delivery System	Features	Characterization	Pharmacokinetics/Tissue Distribution/Efficacy	Ref., Year
Tax and CUR co-loaded MSN	Efficient	Mean Size = (115 ± 15) nm, EE = MTX/CUR: (77.48 ± 2.73)/ (30.70 ± 3.56) %	Pharmacokinetic parameters: Tax-CUR-PLMSN/Tax-CUR-solution (Tax/CUR: 3/18 mg/kg, *iv.*) a. Tax: C_{max}, AUC, $t_{1/2}$, MRT ↑, Vd, CL ↓ b. CUR: C_{max}, AUC ↑, Vd, $t_{1/2}$, CL, MRT↓; In vivo NIR fluorescence real-time imaging (*iv.*): tumor > heart, liver, spleen, lung and kidney; 4T1 tumor inhibition rate: Tax-CUR-PLMSN (*iv.*) = 58.4%, Tax-CUR-PLMSN (*pi.*) = 58.3%, Tax-CUR = 17.3%; 7364 cells (CUR: IC_{50} = 53.16 μM, Tax: IC_{50} = 0.19 μM, Tax-CUR-PLMSN exhibits the strongest cytotoxic effect on BC cells)	2018[103]
CUR conjugated gold nanoparticles	1. Small size 2. High DL 3. Low cytotoxicity	Size = (~ 15 nm)	MCF7 cells viability (25 μg/mL, CUR/nanoparticles: 45/43%); MCF7 cells (cell apoptosis: nanoparticles = 45.57%); MCF7 cells (p-AKT, p-STAT3 ↓, Cleaved PARA ↑); MDA-MB 231 tumor: tumor volume and weight decreased significantly in the group treated with nanoparticles (20 mg/kg, *ip.*) when compared to the control group.	2018[104]
Tax and CUR co-loaded gold nanoparticles	Efficient	Mean Size = (128 ± 10) nm, PDI = (25.5 ± 1.2), zeta potential = (−3.0 ± 1.1) mV	Combined CUR and Tax treatment exerted better cytotoxicity in MDA-MB 231 and 4T1 cell lines without any cytotoxic effect on normal cell lines (HEK-293); MDA-MB 231 cells (cell apoptosis: CUR/Tax/CUR-Tax/Au-C/Au-P/Au-CP = 34.73/23.1/65.07/50.79/33.63/73.56%); 4T1 cells (cell apoptosis: CUR/Tax/CUR-Tax/Au-C/Au-P/Au-CP = 31.06/24.41/50.08/44.15/34.56/72.28%); MDA-MB 231 and 4T1 cells (VEGF, STAT3, Cyclin D ↓, Caspase 9 ↑); 4T1 tumor: mice treated with CUR and CUR-Tax combination showed significant tumor reduction compared to control and Tax treated mice, and the use of AuNP increased treatment efficacy in all groups.	2022[105]
CUR-loaded O/W nanoemulsions	Simple process	Mean Size = (33 ± 3) nm, zeta potential = (+5.0 ± 0.05) mV	-	2021[106]
CUR-loaded self-nanoemulsifying drug delivery systems	1. Efficient 2. High DL	Mean Size = (28.53 ± 0.18) nm, PDI = 0.129, zeta potential = (−22.17 ± 2.90) mV, Equilibrium Solubility = CUR (20.695 ± 0.052) mg/g	MCF7 cells (24 h, CUR: IC_{50} = (6.67 ± 0.5) μg/mL, nanoparticles: IC_{50} = (4.76 ± 0.3) μg/mL)	2020[107]

CUR-loaded exosomes	Good biocompatibility	Mean Size = (84 ± 7) nm, PDI = (0.19 ± 0.02), DL = (18–24) %, EE = (53.9 ± 6.7) %	Tissue distribution: targeting efficiency in liver, brain, lung ↑; MDA-MB-231 cells inhibition rate (72h, CUR: 10–35%, exosomes: 70–80%); MDA-MB-231 cells (TNFα ↓)	2017[108]
CUR-loaded exosomes	Good biocompatibility	Mean Size = (184.7 ± 13.2) nm	Pharmacokinetic parameters: Free CUR (41 ± 15 μM) peaked in breast tissue 6 minutes after EXO-CUR administration, and free CUR was not detected in breast tissue at any of the test times after free CUR administration; MCF7 and MDA-MB-231 cells inhibition rate (72h, exosomes > CUR); MCF7 cells (cell apoptosis: exosomes > CUR); MCF7 cells (Caspase 3, Caspase 9 ↑)	2022[109]
CUR-loaded LLN	High uptake rate	Mean Size= (169 ± 4) nm, PDI= (0.19 ± 0.05)	MCF-7 cells (72 h, CUR: IC_{50} = (3.4 ± 0.2) μM, LLN: IC_{50} = (4.3 ± 0.2) μM)	2018[110]
GO-CUR and GQDs-CUR	Efficient	a. GO-CUR b. GQDs-CUR Mean Size = b: (170 ± 30) nm, zeta potential = a: (−13.5 ± 0.8) mV, b: (−1.2 ± 0.3) mV, DL = a: (80 ± 1) %, b: (83 ± 1) %	MCF-7 cells (48 h, GO-CUR: IC_{50} = (8 ± 0.5) μg/mL, GQDs-CUR: IC_{50} = (5.5 ± 0.5) μg/mL); MDA-MB-231 (48 h, GO-CUR: IC_{50} = (4.8 ± 0.5) μg/mL, GQDs-CUR: IC_{50} = (2.8 ± 0.5) μg/mL)	2020[111]

https://doi.org/10.2147/IJN.S410688

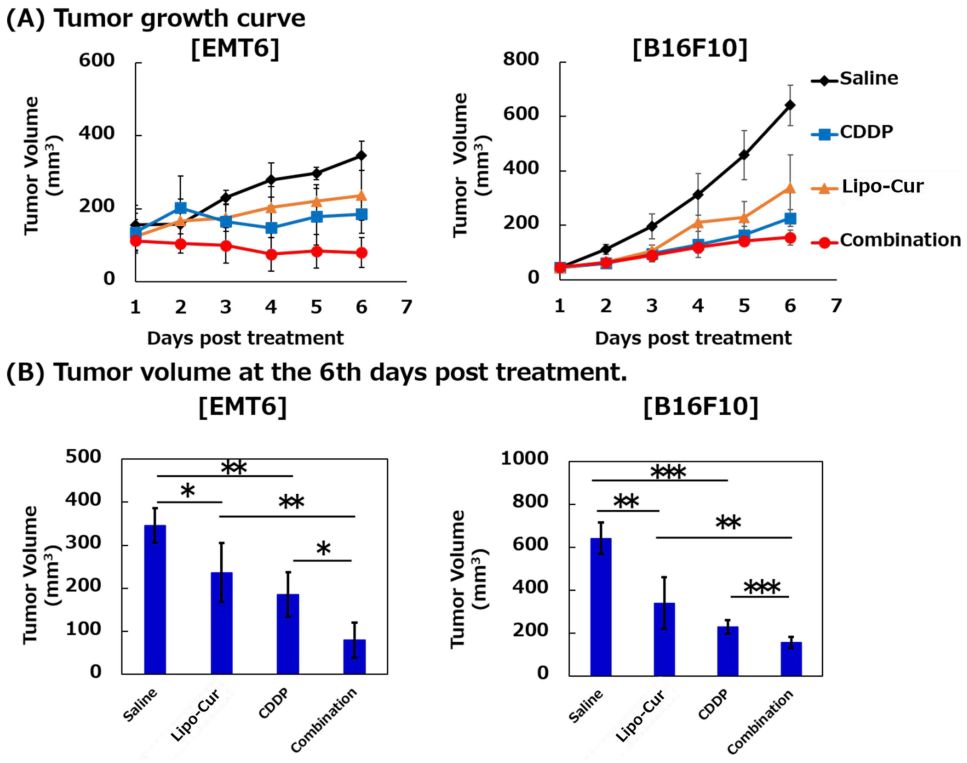

Figure 6 In vivo efficacy of different treatments against EMT-6 and B16F10 tumor models. (**A**) Tumor growth kinetics and (**B**) tumor volume on day 6. Tumor-bearing mice were injected with saline, Lipo-Cur (20 mg/kg), cisplatin (CDDP: 15 mg/kg), or combination (Lipo-Cur + CDDP) on day 0. Data = mean ± S.D (n=5). *p < 0.05, **p < 0.01, ***p < 0.005. Reproduced with permission from Hamano N, Böttger R, Lee SE, et al. Robust microfluidic technology and new lipid composition for fabrication of curcumin-loaded liposomes: effect on the anticancer activity and safety of cisplatin. *Mol Pharm*. 2019;16(9):3957–3967.[89] Copyright 2019, American Chemical Society.

chitosan. These results show the possibility of using coated nanoliposomes made from marine and plant sources as a regulated medication delivery system for the treatment of BC. Moreover, Li et al[91] synthesized mercaptan-derived chitosan (CSSH) and applied it to the coating of liposomes. The EE of CUR liposomes coated with CSSH (CUR-Lip-CSSH) was 93.95%, the DL was 7.95%, the average particle size was 406.0 nm, and the positive zeta potential was 36.6 mV, which were higher than those of the uncoated liposomes. At pH 5.5 and pH 7.4, CUR-Lip-CSSH showed slower in vitro release than uncoated liposomes.

In addition, multidrug combinations tend to demonstrate better efficacy than monotherapy.[113] Multidrug combination therapy can act on multiple pathways and multiple targets at the same time, providing synergistic antitumor effects, reducing toxic side effects associated with single drugs, and overcoming treatment-related multidrug resistance, among other benefits.[114–116] Mahmoudi et al[92] inserted CUR into the bilayer membrane of DDP liposomes to obtain a dosage-controlled codelivery agent that can induce apoptosis of BC cells. Response surface methodology (RSM) was used to optimize the concentrations of CUR and DDP in nanoliposomes, and the results revealed 99.81% and 23.86% EE of CUR and DDP, respectively. The cytotoxicity assessment of various CUR-DDP-NLP concentrations showed concentration dependence. Compared with free drugs and DDP liposomes (DDP-NLP), CUR-DDP-NLP significantly reduced the activity of BC cells (82.5%) when the final concentrations of CUR and DDP were 32 μg/mL and 20 μg/mL, respectively. Furthermore, flow cytometry demonstrated that CUR-DDP-NLP caused almost ten times more apoptosis than DDP-NLP. With the potential to encapsulate and release both hydrophobic and hydrophilic drugs, this codrug delivery system has the advantages of lowering cytotoxicity and achieving high efficacy.

Micell-Based CUR Delivery

In recent years, polymeric micelles have been widely used in preclinical studies for the delivery of microsoluble or insoluble chemotherapeutic drugs in cancer therapy, and polymeric micelles have become a potential drug delivery system.[117] Compared with vesicles composed of lipids, micelles are nanosmall, monodisperse, relatively stable and

economical, and can be surface modified or stimulated to sensitize by modulating their chemical structure.[118,119] Due to their smaller size compared to other lipid carriers, polymeric micelles can prevent uptake by the reticuloendothelial system through enhanced permeability and retention effects, resulting in a prolonged half-life of polymeric micelles in the blood and enhanced aggregation of micelles into the tumor microenvironment.[120,121]

Karabasz et al[93] synthesized an alginate CUR conjugate (AA-CUR) that formed stable micelles. The estimated amount of CUR in 1 g of AA-CUR conjugate was 45 mg, and AA-CUR had good solubility in water (7 mg/mL). AA-CUR had an average particle size of 205 nm, a critical micelle concentration (CMC) of 0.654 mg/mL, and a zeta potential of −53 mV. The tested AA-CUR was nontoxic and safe but showed only moderate antitumor efficacy, according to the results of in vivo toxicity and antitumor activity tests. Furthermore, a trifunctionalized amphiphilic polymer composed of α-tocopheryl succinate (α-TOS), cholesterol and polyethylene glycol, in which the three parts are linked together by a trifunctional group lysine, was synthesized by Muddineti et al.[94] Due to the presence of two compatible lipid components, the newly designed polymer has a larger lipid core for improved drug delivery. It is also biocompatible and biodegradable and exhibits synergistic anticancer activity by inducing a-TOS-mediated apoptosis and multidrug resistance inhibition. The process was optimized to prepare micelles with a DL of 14.2 ± 0.24%, EE of 98.6 ± 1.48%, and mean particle size, PDI and zeta potential of 175.8 ± 0.68 nm, 0.248 ± 0.075 and 5.9 ± 0.78 mV, respectively. The micelles prepared in the article serve as a biocompatible and efficient drug delivery system that can deliver insoluble hydrophobic drugs with good DL properties.

Nanogel-Based CUR Delivery

Nanogels with porous structures, good biocompatibility, large surface areas and excellent DL properties are promising drug carriers.[122,123] Sarika et al[95] loaded CUR into gum Arabic aldehyde gelatin nanogels using the inverse miniemulsion technique. The nanogels had a hydrodynamic diameter of 452 ± 8 nm, a zeta potential of −27 mV and an EE of 65 ± 3%. The in vitro anticancer activity was evaluated using MCF-7 cells, and the results showed that 50 μg/mL CUR nanogels were acutely toxic to MCF-7 cells. The toxicity of CUR-loaded nanogels was less toxic at other doses than that of CUR. Furthermore, Nguyen et al[96] prepared an amphiphilic heparin-polyoxyethylene ether P403 (HP403) nanogel using the emulsification solvent evaporation method, which can efficiently coload CUR and DDP hydrate (CisOH) by two loading mechanisms (HP403@CisOH@CUR). In comparison to neutral pH, the release rate of CUR and CisOH was accelerated at pH 5.5, demonstrating efficient transport of the drugs to the tumor site. HP403@CisOH@CUR nanogels significantly inhibited MCF-7 cells in vitro, and in mice, in vivo tests revealed that the dual drug platform extended survival duration and prevented tail necrosis. In summary, HP403@CisOH@CUR offers an intriguing method for combining the anticancer benefits of DDP and CUR on a well-designed delivery platform while avoiding the drawbacks of DDP in BC treatment.

Nanoparticle-Based CUR Delivery

Solid lipid nanoparticles (SLNs) are a new drug delivery system made by embedding or encapsulating drugs in lipid materials. Most of the carriers are solid natural or synthetic lipids with low toxicity, excellent degradability and good compatibility. To increase the half-life of pharmaceuticals, minimize drug degradation, and lessen leakage, SLNs are frequently utilized as drug delivery systems for poorly soluble medications. Wang et al[97] loaded CUR into SLNs to improve its therapeutic effect on BC. The test findings demonstrate the good spherical structure of CUR-SLNs. The size was approximately 40 nm, and the zeta potential was −25.3 ± 1.3 mV. The DL and EE of SLN were 23.38% and 72.47%, respectively. CUR-SLNs have strong cytotoxicity to SKBR3 cells. A significant absorption efficiency of CUR-SLN was observed in SKBR3 cells in an in vitro cell uptake investigation. Furthermore, SKBR3 cells treated with CUR-SLNs induced more apoptosis than those treated with free CUR. In addition, Abd Ellate et al[98] prepared two kinds of biocompatible SLNs loaded with CUR (with or without chitosan coating) to increase stability, uniform water dispersion and cell uptake. SLN loaded with CUR is 5–10 times more efficient than free CUR at increasing intracellular retention and doxorubicin (DOX) toxicity in TNBC. Without showing any symptoms of systemic toxicity, the SLN loaded with CUR also successfully preserved the sensitivity of DOX-resistant TNBC tumors. These findings suggest that overcoming chemotherapeutic resistance in TNBC can be accomplished safely and effectively by combining CUR-loaded SLN with DOX.

Polymer nanoparticles are carriers prepared from biocompatible and biodegradable polymers with a particle size range of (10–1000) nm. They have the advantages of higher EE and structural stability and can be endowed with more functions through

structural modification, so they have higher bioavailability and efficacy.[124,125] Numerous polymers, including poly (lactic-co-glycolic acid) (PLGA) and chitosan, have been utilized to create nanoparticles. Lactic and glycolic acids are randomly polymerized to form PLGA, a biodegradable functional polymer organic molecule. It possesses excellent encapsulation, nontoxicity, biocompatibility, and film-forming capabilities.[126] Meena et al[99] used PLGA as the carrier to prepare positively charged CUR nanoparticles by a nanoprecipitation method. The obtained nanoparticles had a small particle size (81.05 nm), positive charge, high DL (21.8%) and slow release in vitro. In MDA-MB-231 cells, nanoparticles showed higher cytotoxicity than free CUR. Moreover, Vakilinezhad et al[100] prepared and evaluated PLGA nanoparticles for the codelivery of Methotrexate (MTX) and CUR. When compared to free MTX, CUR, or even its independently loaded formulations, the coloaded nanoparticles demonstrated noticeably greater cytotoxicity. MTX and CUR codelivery demonstrated synergistic effects on inhibiting the progression of BC, according to in vivo results. The deacetylation of chitin in the exoskeleton of marine crustaceans generates chitosan, a linear amino polysaccharide with repeating units of d-glucosamine and n-acetyl-d-glucosamine. Because of their excellent biocompatibility and biodegradability, chitosan nanoparticles are often utilized in the field of drug delivery. They can raise the local drug concentration in tumor tissue, decrease drug toxicity, and increase efficacy.[127–129] Abdel-Hakeem et al[101] synthesized chitosan/protamine nanocarriers and used them to encapsulate CUR. Cell-based assays showed that compared with free CUR, after treatment with nanoparticles, cell viability and NF-κB, TNF-α and IL-6 levels were significantly reduced, and the nanoparticles could effectively modulate the expression of Bcl-2 anti-apoptosis genes. Tumor necrosis TRAIL has the characteristic of selective apoptosis in tumor cells and is considered a promising new adjuvant therapy for some cancers, including BC. Furthermore, placental-derived mesenchymal stem cells (PDMSCs) were genetically engineered to deliver soluble TRAIL at tumor sites.[130,131] Therefore, Kamalabadi Farahani et al[102] prepared CUR-loaded chitosan nanoparticles to enhance the apoptosis-promoting effect of TRAIL. The antitumor effects of this combination therapy were investigated in vitro and using BC mouse models. The outcomes demonstrated that concurrent administration of TRAIL-expressing PDMSCs and CUR nanoparticles could successfully cause tumor cell death and considerably slow tumor growth in vivo.

In biomedical research, mesoporous silica nanoparticles (MSNs) have emerged as a key drug delivery technology. The importance of MSNs in drug delivery research is highlighted by their biocompatibility, variable porosity, controlled drug release, high loading capacity, and stability.[132,133] Lin et al[103] prepared highly ordered MSNs with a pore size of 2.754 nm and a particle size of 115 ± 15 nm using an etching method. Homogeneous polyethylene glycolized lipid bilayers with a thickness of 10–15 nm were wrapped around the MSN surface using a thin film hydration method. Afterward, paclitaxel (Tax) and CUR were coencapsulated into PEGylated lipid bilayers of mesoporous silica nanoparticles (PLMSNs). The Box–Behnken method was used to optimize the preparation process, and the final nanoparticle EE of Tax and CUR were 77.48 ± 2.73% and 30.70 ± 3.56%, respectively. The morphometry of the nanoparticles showed that the composite nanoparticles were spherical particles with uniform dispersion. Furthermore, Gao et al[134] further investigated the pharmacokinetic properties, in vivo distribution and tumor accumulation capacity, and therapeutic effects of the above drug delivery system. The results revealed that the AUCs of both drugs were significantly enhanced by the drug delivery system, and both intratumoral and intravenous administration groups had better tumor weight control than the control groups in terms of their anticancer effects.

Gold nanoparticles, as biocompatible high atomic number materials with easily modified surfaces and low in vivo toxicity, have been widely used in tumor therapy and have promising clinical translation prospects.[135,136] Khandelwal et al[104] endeavored to suffix CUR molecules on the surface of gold quantum clusters (Au QC) by a novel in situ synthesis method, which not only provided an alternative pathway to reduce metal content but also to increase the water solubility and DL of CUR. The cytotoxicity results showed lower cytotoxicity of CUR-incorporated Au QC (C-Au QC) to normal cells and almost the same cytotoxicity to cancer cells compared to free CUR, suggesting that CUR retains its anticancer properties even after binding to Au QC. Western blotting analysis demonstrated that C-Au QC induced cancer cell apoptosis. C-Au QC efficiently reduced tumor growth in vivo, according to research, without significantly harming internal organs. In addition, Vemuri et al[105] coloaded CUR with Tax in gold nanoparticles (Au-CP) and evaluated the synergistic anti-metastatic activity of CUR and Tax. In vitro results showed that Au-CP exhibited excellent synergistic cytotoxic effects against TNBC cell lines (MDA-MB 231 and 4T1 cells). Mechanistic studies showed that anticancer effects were associated with downregulation of VEGF, Cyclin-D1 and STAT-3 gene expression and upregulation of the apoptotic Caspase-9 gene. According to in vivo anticancer data, mice treated with the combination of CUR and Tax (with or without gold nanoparticles) had much smaller tumors than mice treated with Tax alone and control groups.

Nanoemulsion-Based CUR Delivery

Nanoemulsions, also known as microemulsions, are thermodynamically stable, transparent or translucent homogeneous dispersion systems formed spontaneously by water, oil, surfactants and cosurfactants, with particle sizes of 1 to 100 nm. Nanoemulsions have the advantages of a straightforward preparation procedure, increases in drug solubility, decreases in drug enzymatic dissolution in the body, a protective effect on medications, enhancements drug absorption in the gastrointestinal system, enhancements of drug bioavailability, etc.[137–140] Bharmoria et al[106] developed a biomaterial that is compatible with CUR and has a suitable structure. The developed biomaterial started by preparing an oil-in-water nanoemulsion using a cytocompatible copolymer (Pluronic F 127) coated with a positively charged protein (gelatin) designed as G-Cur-NE. The results showed that G-Cur-NE enhances the stability of CUR and improves its bioaccessibility. Moreover, Kazi et al[107] developed an oral lipid-based bioactive self-emulsifying drug delivery system (Bio-SNEDDS) for CUR as a drug candidate for cancer therapy. Representative Bio-SNEDDS (Black Seed Oil/Imwitor 988/KolliphorEL (35/15/50) % w/w) showed a smaller droplet size (28.53 nm), higher DL, and a clear appearance after aqueous dilution. Dynamic dispersion and in vitro lipolysis data demonstrated that Bio-SNEDDS was able to maintain CUR in soluble form in the gastrointestinal tract, and MTT assays showed that representative Bio-SNEDDS treatment resulted in reduced cell viability of MCF-7 cells compared to free CUR and conventional SNEDDS.

Active Targeting Agent

Active TDDs refer to agents in which the drug carrier is capable of molecularly specific interactions with the target tissue.[141] Proteins, antibodies, peptides, or small chemical compounds are commonly used as ligands to modify the drug delivery system's surface and enable targeted drug administration by binding to surface antigens or receptors expressed in tumor tissues (Figure 7).[142] The goal of active targeting is to raise the local concentration of drug nanocarriers at the tumor location as opposed to healthy tissues and to assist in the internalization of the complex by tumor cells.[143] Researchers have created a wide range of CUR-loaded active TDDSs to increase CUR effectiveness and reduce its toxicity and adverse effects.[144] The active TDDSs of CUR are summarized in Table 3.

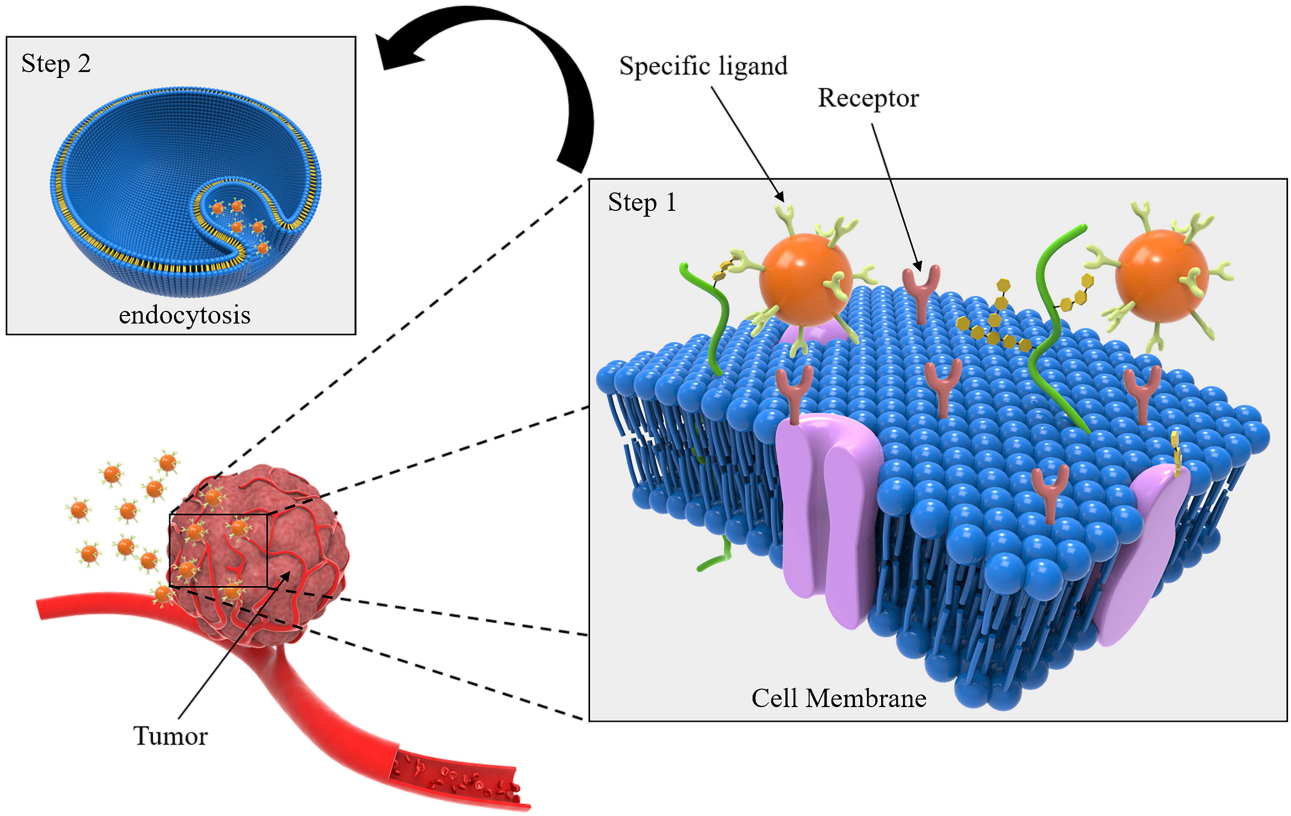

Figure 7 Specific ligands are used to modify the surface of the drug delivery system to specifically bind to surface antigens or receptors expressed in tumor tissue, thereby triggering endocytosis of tumor cells and enabling targeted drug delivery.

Table 3 Active TDDS of CUR

Drug Delivery System	Ligand/Antibody	Receptor/ Antigen	Efficacy	Ref., Year
PEI-PEG-CUR-liposomes	Branched polyethylenimine (PEI)	HER2	Targeting efficiency: Ability of the DiO-LPPC/Herceptin complex to interact with various BC cells with different levels of HER2 surface expression: SKBR-3 cells ($HER2^{++}$) > MCF7 cells ($HER2^{+}$) > MDA-MB-231 cells ($HER2^{-/+}$) > Hs578T cells ($HER2^{-}$); In vivo NIR fluorescence real-time imaging (*iv.*): SKBR-3 tumor > heart, liver, spleen, lung and kidney; SKBR-3 cells (CUR: IC_{50} = (15.73 ± 3.7) μM, CUR/LPPC: IC_{50} = (1.28 ± 0.14) μM, CUR/LPPC/Herceptin: IC_{50} = (0.23 ± 0.01) μM); MCF-7 cells (CUR: IC_{50} = (10.21 ± 1.13) μM, CUR/LPPC: IC_{50} = (0.96 ± 0.23) μM, CUR/LPPC/Herceptin: IC_{50} = (0.27 ± 0.09) μM); MDA-MB-231 cells (CUR: IC_{50} = (12.15 ± 5.23) μM, CUR/LPPC: IC_{50} = (1.23 ± 0.12) μM, CUR/LPPC/Herceptin: IC_{50} = (0.57 ± 0.03) μM); Hs578T cells (CUR: IC_{50} = (12.46 ± 1.65) μM, CUR/LPPC: IC_{50} = (0.87 ± 0.07) μM, CUR/LPPC/Herceptin: IC_{50} = (0.59 ± 0.06) μM); SKBR-3 tumor inhibition rate (*iv.*, once every 3 days): CUR/LPPC/Herceptin (40 mg/kg CUR, 4 mg/kg Herceptin) = 94%, CUR-H/LPPC/Herceptin (200 mg/kg CUR, 4 mg/kg Herceptin) = 100%	2019[145]
HER2 aptamer-decorated CUR-loaded human serum albumin nanoparticle (Apt-HSA/CURNP)	HER2-bonding aptamer (HB5)	HER2	Cellular uptake (SK-BR3 cells > MCF-7 cells); SK-BR3 cells viability (72h, CUR > Apt-HSA/CUR NP); MCF-7 cells viability (72h, CUR < Apt-HSA/CUR NP)	2019[146]
Fab'-CUR-NPs	Fab' (an antigen-binding fragment cut from trastuzumab)	HER2	Cellular uptake (BT-474 cells ↑); BT-474 cells viability (48h, CUR > CUR-NPs > TMAB-CUR-NPs > Fab'-CUR-NPs)	2018[147]
GE11-CUR-NPs	GE11	EGFR	Cellular uptake (MCF-7 cells ↑); MCF-7 cells (cell apoptosis: CUR = 11%, CUR-NPs = 14.9%, GE11-CUR-NPs = 18.9%; PI3K, P-Akt ↓); MCF-7 cells viability (24h, CUR > GE11-CUR-NPs); MCF-7 tumor inhibition rate: GE11-CUR-NPs (5 mg/kg, *iv.*, once a day, 20 times) > CUR-NPs (5 mg/kg, *iv.*, once a day, 20 times) > CUR (5 mg/kg, *iv.*, once a day, 20 times)	2017[148]
HA-CUR-MSN	HA	CD44	Cellular uptake (MDA-MB-231 and MCF7 cells ↑); MDA-MB-231 cells (48 h, CUR-MSN: IC_{50} = 213.03 μg/mL, HA-CUR-MSN: IC_{50} = 82.98 μg/mL); MDA-MB-231 cells (cell apoptosis ↑; NF-κB ↓, Bax, Cleaved caspase 3 ↑); Ex-vivo optical imaging (*iv.*): tumor > kidney > heart, lung; EAC tumor inhibition rate: HA-CUR-MSN (67.75 mg/kg, *iv.*, every other day for 2 weeks) > CUR-MSN (60.79 mg/kg, *iv.*, every other day for 2 weeks)	2021[149]
HA coated Pluronic F127/ didecyldimethylammonium bromide (PD) mixed nanomicelles	HA	CD44	MDA-MB-231 cells (48 h, CUR: IC_{50} = 4.11 μg/mL, CUR-PD micelles: IC_{50} = 3.20 μg/mL, CUR-HA-PD micelles: IC_{50} = 2.83 μg/mL)	2021[150]

HA/TN liposomes	HA	CD44	Cellular uptake (4T1 and RAW cells ↑); 4T1 cells (HA/TN-CCLP: IC_{50} = 12.3 μM); RAW cells (HA/TN-CCLP: IC_{50} = 9.2 μM); HUVEC cells (HA/TN-CCLP: IC_{50} = 270.0 μM); 4T1 cells (cell apoptosis: TN-CCLP = 27.12%, HA/TN-CCLP = 25.12%, cell migration ↓); Ex-vivo optical imaging (*iv.*): tumor ↑; 4T1 tumor inhibition rate: TN-CCLP (20 mg/kg, *iv.*, 9, 12, 15, 18 day) = 41%, HA/TN-CCLP (20 mg/kg, *iv.*, 9, 12, 15, 18 day) = 55%	2019[151]
HA-PEG-PLGA NPs	HA	CD44	Cellular uptake (MCF7 cells ↑); MCF7 cells (proliferation ↓, migration ↓; Vimentin ↓, E-cadherin ↑)	2020[152]
RGD-modified liposomes	RGD	$\alpha_v\beta_3$	MCF7 cells viability (72h, 32 μg/mL, RGD-Lip-Cur = (18.39 ± 4.02) %); MCF7 cells (cell apoptosis: CUR = 46.64%, Lip-Cur = 76.86%, RGD-Lip-Cur = 79.8%)	2021[153]
Peptide-HSA/CUR NPs	PDL1 binding peptide	PDL1	Cellular uptake (MDA-MB-231 cells ↑); MDA-MB-231 cells (24/48/72 h, CUR: IC_{50} = 278/259/234 μM, HSA/CUR NPs: IC_{50} = 261/157/126 μM, peptide-HSA/CUR NPs: IC_{50} = 249/100/61 μM); MCF7 cells (24/48/72 h, CUR: IC_{50} = 50/47/55 μM, HSA/CUR NPs: IC_{50} = 40/35/30 μM, peptide-HSA/CUR NPs: IC_{50} = 45/42/31 μM); SKBR-3 cells (24/48/72 h, CUR: IC_{50} = 396/199/167 μM, HSA/CUR NPs: IC_{50} = 173/78/69 μM, peptide-HSA/CUR NPs: IC_{50} = 181/71/54 μM); MDA-MB-231 cells (cell apoptosis: CUR = (25.2 ± 1.9) %, HSA/CUR = (28.6 ± 1.14) %, peptide-HSA/CUR NPs = (43.4 ± 2.7) %)	2020[154]
FA-CUR lipid nanoparticles	FA	FA receptor	MCF7 cells (CUR: IC_{50} = (18.23 ± 2.56) μg/mL, CUR-NLC: IC_{50} = (6.16 ± 0.67) μg/mL, FA-CUR-NLC: IC_{50} = (1.75 ± 0.29) μg/mL); MCF7 tumor inhibition rate: CUR (*iv.*, 0, 3, 6, 9, 12, 15 day) = 31%, CUR-NLC (*iv.*, 0, 3, 6, 9, 12, 15 day) = 66%, FA-CUR-NLC (*iv.*, 0, 3, 6, 9, 12, 15 day) = 83%	2016[155]
CUR-loaded chitosan nanoparticles	FA	FA receptor	MCF7 cells viability (nanoparticle < CUR)	2017[156]
CUR-loaded microspheres	FA	FA receptor	Cellular uptake (MDA-MB-468 cells ↑); MDA-MB-468 cells (microsphere: LD_{50} =45 μM); 4T1 cells (microsphere: LD_{50} = 40 μM)	2019[157]
Tf-PEG-CUR/DOX NPs	Transferrin	Transferrin receptor	MCF7 cells (72 h, Tf-PEG-CUR/DOX NPs: IC_{50} of CUR = (2.6 ± 0.3) μM, IC_{50} of DOX = (2.6 ± 0.3) μM); MCF7 tumor inhibition rate: Tf-PEG-CUR/DOX NPs (*iv.*, once a week for 7 weeks) = 83.5%	2017[158]

https://doi.org/10.2147/IJN.S410688 DovePress

Human Epidermal Growth Factor Receptor 2 (HER2 Receptor)

Approximately 25% of invasive BCs have HER2 overexpression; however, its expression is at its lowest in normal adult tissue.[159] Trastuzumab, a humanized monoclonal antibody that targets the HER2 receptor, is now the treatment of choice for HER2-positive BC. HER2 has been considered a viable target for the targeted delivery of nanoparticles to BC because of its increased expression on tumor cells, extracellular accessibility, and internalization upon antibody interaction.[160] Based on this, Lin et al[145] designed a CUR-loaded cationic liposome-PEG-PEI complex (LPPC) for targeted drug delivery to HER2-expressing BC cells. The branched polyethyleneimine (PEI) in LPPC provides a positive charge from its amine moiety through electrostatic interactions to associate with the carboxyl group of the antibody. The branched PEI not only provides a positive charge to associate with the antibody but also prepares a dense mesh with PEG to immobilize the protein on the surface of the LPPC. The average size of the drug-loaded LPPC was approximately 250 nm, and the zeta potential was approximately 40 mV. Herceptin was complexed to the surface of LPPC to form a drug/LPPC/herceptin complex. The CUR/LPPC/Herceptin complex had a size of 280 nm and a zeta potential of approximately 23 mV. Specific binding on the cell surface and in vivo IVIS pictures that showed specific binding in HER2-positive SKBR3 cells compared to HER2-negative Hs578T cells provided evidence of this delivery system's targeting capacity. The cytotoxic activity of cancer cells was significantly elevated only by the drug/LPPC/Herceptin complex. The immune complex was directed to HER2/neu-positive cells by Herceptin adsorbed on LPPC but not to HER2/neu-negative cells, according to both in vitro and in vivo data (Figure 8). The results show that LPPC can be targeted for BC

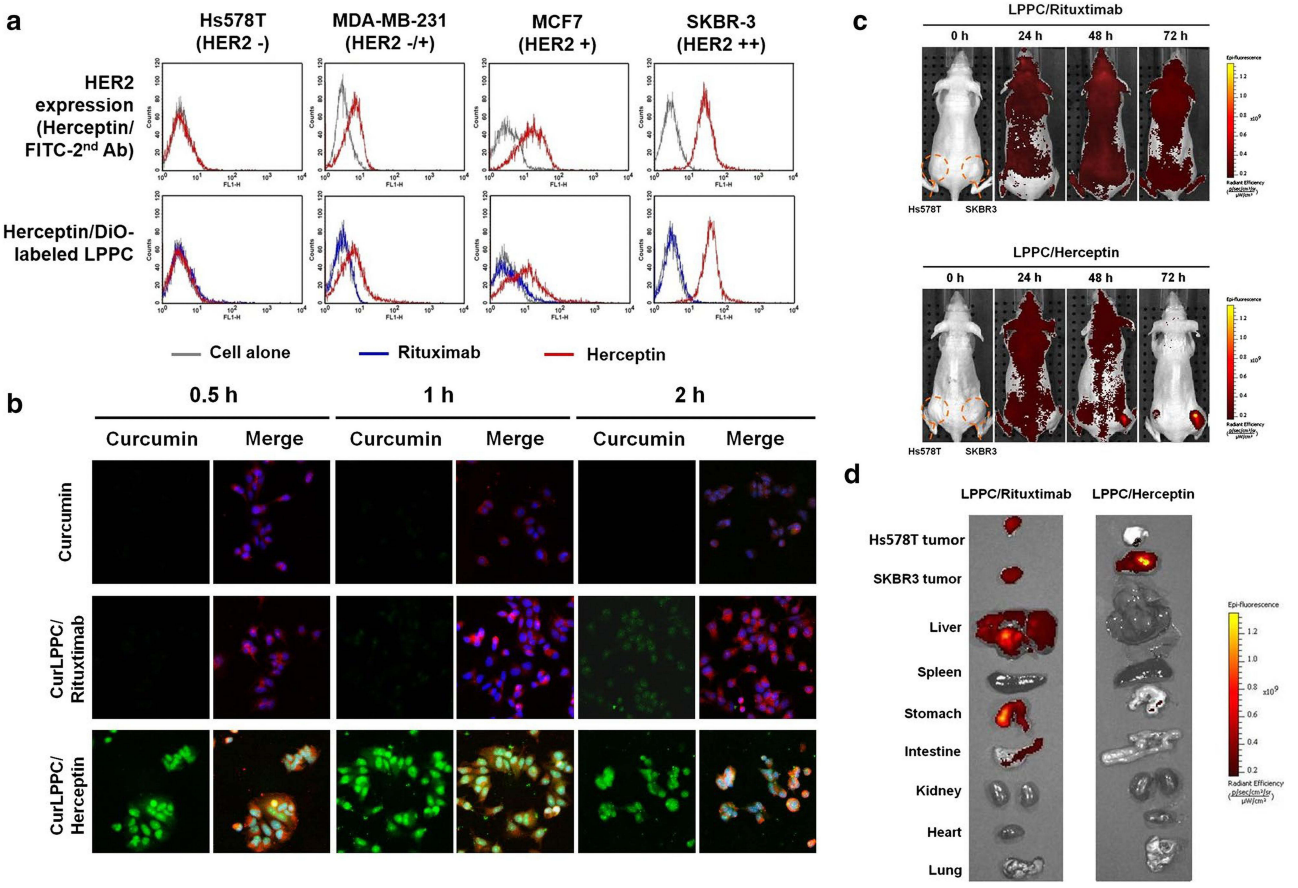

Figure 8 Targeting ability of the drug-loaded immunolipoplex. a The effect of antibody association with immunocomplexes on cell targeting in vitro. The HER2/neu receptor expressed on different cancer cell lines were indirectly probed with the humanized antibodies, Herceptin or Rituximab, and FITC-conjugated goat anti-human IgG antibody. Herceptin or Rituximab were adsorbed on DiO-labeling LPPC to monitor their ability to target BC cell lines when associated with LPPC complexes. b The intracellular accumulation of CUR. MCF-7 cells were treated with CUR, CUR/LPPC/Rituximab or CUR/LPPC/Herceptin at equal concentrations of CUR. The cell membranes were stained with red fluorescent dye DiI, the nuclei were stained with DAPI, and the cellular distribution of CUR is shown as green fluorescence signal. The cells were imaged using a confocal microscope. c Targeting ability of LPPC in vivo. DiI-labeled LPPC/Rituximab or DiI-labeled LPPC/Herceptin complexes were *i.v.* injected into athymic nude mice bearing HER2-negative Hs578T cell and HER2-positive SKBR3 cell-induced tumors. The images were obtained by IVIS at 0, 24, 48 and 72 h after injection. The photon counts of each mouse are indicated by the pseudo-color scales. d After 72 h, the organs and tumors isolated from the treated nude mice were imaged by IVIS. Reproduced with permission from Lin Y-L, Tsai N-M, Chen C-H, et al. Specific drug delivery efficiently induced human breast tumor regression using a lipoplex by non-covalent association with anti-tumor antibodies. *J Nanobiotechnology.* 2019;17(1):25. Creative Commons.[145]

treatment, demonstrating important clinical implications. Saleh et al[146] developed a HER2-adapted CUR-loaded human serum albumin nanoparticle (Apt-HSA/CCM NP) for targeted delivery to HER2-overexpressing BC cells. The obtained nanoparticles had a hydrodynamic diameter of 281.1 ± 11.1 nm and a zeta potential of −33.3 ± 2.5 mV. The data showed a 400-fold increase in water solubility by desolvation of CUR encapsulated in the nanoparticles. Fluorescence microscopy images showed significantly increased cytoplasmic uptake of Apt-HSA/CCMNPs in HER2-overexpressing SK-BR-3 cells compared to their unconjugated counterparts. In both HER2-positive and HER2-negative cell lines, cytotoxicity experiments found no appreciable difference in the cytotoxic effects of free CUR and nontargeted HSA/CCMNPs. However, the toxicity of Apt-HSA/CCMNPs was significantly higher. These findings imply that this targeted delivery method might be a potentially effective therapy option for cancer cells that are HER2-positive. A promising method for delivering actively targeted drugs to tumors uses nanoparticles modified with bioligands. Trastuzumab (TMAB), among other targeting ligands, has a high molecular weight, which restricts its use in targeting.[161,162] Duan et al[147] prepared Fab' (an antigen-binding fragment cut from TMAB)-modified nanoparticles (Fab'-NPs) loaded with CUR as a model drug. The average particle size of the Fab'-CUR-NPs was 128.5 ± 1.3 nm, with a PDI of 0.125 ± 0.012, and the EE was 79.5 ± 1.56%. In vitro cytotoxicity tests revealed that Fab'-CUR-NPs were significantly more effective at killing BT-474 cells that overexpressed the HER2 protein than TMAB-CUR-NPs. Studies on the qualitative and quantitative uptake of Fab'-NPs in BT-474 ($HER2^{+}$) cells revealed that they accumulated more than TMAB-NPs; however, there was no significant difference in MDA-MB-231 ($HER2^{-}$) cells. Additionally, in vivo research revealed that Fab'-CUR-NPs accumulated more in tumors than TMAB-Cur-NPs.

Epidermal Growth Factor Receptor (EGFR)

A membrane surface sensor with tyrosine kinase activity, known as the EGFR, is a member of the ErbB receptor family. It is frequently expressed in human epidermal and stromal cells and is highly expressed in a number of human malignancies, including non-small cell lung cancer and BC.[163,164] To determine the type of malignant tumor, the EGFR gene can be checked for mutations, and subsequently targeted therapy can be performed.[165,166] Jin et al[148] prepared CUR-loaded GE11 peptide-modified PLGA nanoparticles (GE11-CUR-NPs). GE11 specifically binds EGFR, has high affinity for high EGFR-expressing tumor cells and is currently the most widely used nonnatural targeting peptide for targeted tumor research. The average particle size of GE11-CUR-NPs was 210 ± 54 nm, the zeta potential was −22 ± 3.6 mV, the PDI was 0.112 ± 0.019, and the EE was 92.3 ± 2.7%. GE11-CUR-NPs could effectively deliver the anticancer agent CUR to EGFR-expressing MCF-7 cells in vitro and in vivo. When compared to free CUR, GE11-CUR-NP treatment of BC cells and tumor-bearing mice reduced phosphatidylinositol 3 kinase signaling, decreased cancer cell viability, and slowed drug removal from the circulation.

CD44

CD44 is a complex transmembrane adhesion glycoprotein that is normally overexpressed on BC cells and is involved in tumorigenesis, progression and metastasis.[167,168] The N-terminal end of the CD44 peptide chain can bind hyaluronic acid (HA), so CD44 is also considered a receptor for hyaluronic acid.[169] Based on this, Ghosh et al[149] achieved the targeted delivery of CUR in cancer cells by binding HA on the surface of MSNs. HA-CUR-MSN has a diameter of approximately 75 nm, a negatively charged surface, and a DL of 14.76%. By inducing ROS, cell cycle arrest, and regulation of the NF-B- and Bax-mediated apoptosis pathways, it facilitates MDA-MB-231 cell death. Additionally, the enhanced bioavailability and cellular uptake of CUR in tumor tissues allowed HA-CUR-MSNs to successfully reduce tumor volume in tumor-bearing mice in comparison to free CUR. Collectively, the results of this study showed that HA-CUR-MSNs were more effective against cancer than free CUR. Collectively, the results of this study showed that HA-CUR-MSN was more effective against cancer than free CUR. Soleymani et al[150] prepared a facile method of HA-modified hybrid nanomicelles containing CUR to provide an effective drug delivery system for targeted therapy of high CD44 receptor-expressing BC cells. The DL and EE of CUR-HA-PD micelles were 2.8% and 95.1%, respectively. The average hydrodynamic dimensions of the prepared nanomicelles before and after encapsulation with HA were 19.8 and 35.8 nm, respectively. Compared to CUR-PD micelles and free CUR, CUR-HA-PD micelles were found to have increased cytotoxicity to MDA-MB-231 cells in an in vitro cytotoxicity assay. It appears that CUR-HA-PD micelles have potential as a targeted anticancer drug delivery system. Moreover, Sun et al[151] prepared a novel liposome (HA/TN-CCLP) modified with TN

(TAT-NBD peptide, NF-κB essential modulator (NEMO)-binding domain peptide (NBD) and cell-permeable peptide (TAT) that selectively blocks the NF-κB activation pathway, leading to tumor growth inhibition) and HA-coated with coloaded CUR and celecoxib (Figure 9). HA/TN-CCLP had a mean particle size of 126.90 ± 8.30 nm and a zeta potential of −24.10 ± 1.10 mV. The DLs of CUR and celecoxib were 2.32 ± 0.10% and 1.86 ± 0.10%, respectively, and the EEs were 89.50 ± 1.70% and 91.40 ± 1.00%, respectively. In vitro experiments revealed that TN-CCLP performed better than HA/CCLP. Contrary to the in vitro data, HA/TN-CCLP had the longest circulation time and the strongest tumor aggregation, which led to the most substantial anti-inflammation, inhibition of macrophage recruitment, and antitumor effects after systemic therapy in 4T1 mammary holotype mice. In particular, HA/TNCCLP has the potential to prevent BC metastases to the lungs. In conclusion, by enhancing inflammatory infiltration of tumor tissue, the new CD44-targeted TN-CCLP has the potential to prevent the growth and metastasis of tumors. In addition, Zhao et al[152] prepared HA-modified PLGA nanoparticles coloaded with CUR and salinomycin. To reduce therapeutic resistance and cause cell death, the therapeutic drugs CUR and salinomycin perform complementary roles. Upon binding to HA, the hydrodynamic size of the nanoparticles increased from 120.1 ± 5.5 to 153.4 ± 4.6 nm. The surface charge also exhibited negative zeta potential values upon HA conjugation. The DL of salinomycin and CUR in the nanoparticles was approximately 70% and 82%, respectively. According to the results, coloaded nanoparticles can efficiently cause cell death as well as prevent cell migration and attachment. This is likely due to a mechanism that prevents the G1 phase of the cell cycle from progressing, which causes cell cycle arrest and the subsequent induction of apoptosis in BC cells.

Integrin $\alpha_v\beta_3$

Because BC, lung cancer, and activated vascular endothelial cells express the integral protein $\alpha_v\beta_3$ at high levels, whereas other endothelial cells and the majority of noncancerous cells express it at low or no levels, this protein is a possible option for targeted drug delivery.[170–172] The arginine-glycine-aspartate (RGD) tripeptide has a strong affinity for $\alpha_v\beta_3$.[173] RGD-conjugated nanoparticles can deliver chemotherapeutic drugs to BC cells through $\alpha_v\beta_3$ integrin recognition.[174,175]

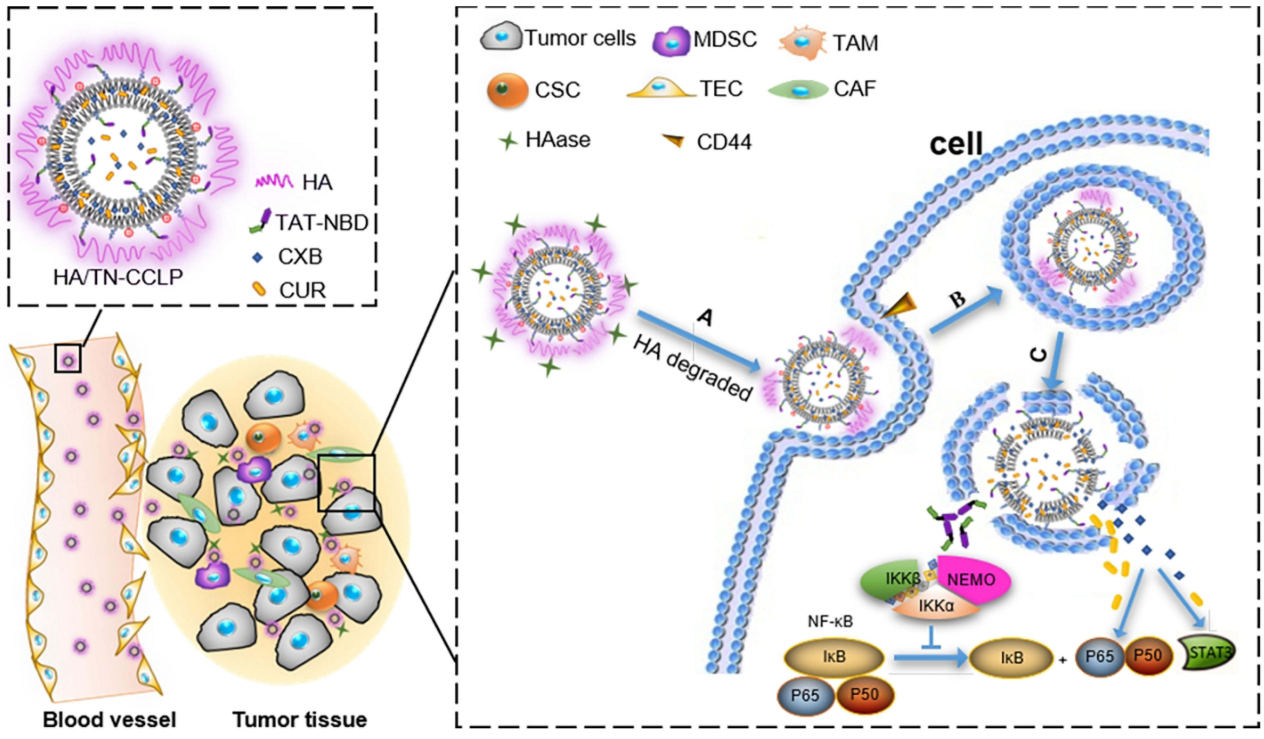

Figure 9 Schematic illustration of the in vivo fate of HA/TN-CCLP. After intravenous injection, HA/TN-CCLP preferentially accumulate at the tumor tissues. (**A**) HA shell degraded or partially degraded by HAase, exposed TN-modified cationic liposome and CD44 receptor promoted cellular uptake; (**B** and **C**) Endo-lysosomal escape. The released CXB, CUR and TN acted on NF-κB and STAT3. Reproduced with permission from Sun Y, Li X, Zhang L, et al. Cell permeable NBD peptide-modified liposomes by hyaluronic acid coating for the synergistic targeted therapy of metastatic inflammatory breast cancer. *Mol Pharm*. 2019;16(3):1140–1155.[151] Copyright 2019, American Chemical Society.

Mahmoudi et al[153] encapsulated CUR into RGD-modified liposomes (RGD-Lip-Cur). The average particle size of RGD-Lip-Cur was 97.4 ± 7.1 nm, and the EE reached 99.5%. In comparison to Lip-Cur and CUR, the MTT assay revealed that RGD-Lip-Cur had a significantly greater cytotoxic effect on MCF-7 cells at doses of 32, 16, and 4 μg/mL. The data show that the RGD-Lip-Cur vector is novel and has a potent cytotoxic effect against the BC cell line.

PDL1

Under physiologically induced inflammation, the immune response is regulated by the immunological checkpoint protein known as Programmed Death Ligand 1 (PDL1).[176] However, it has been demonstrated that chemotherapy and radiation therapy can induce or increase the expression of this ligand in a number of tumor types, including BC.[177] Cancer cells have the ability to deplete T cells and suppress the immune response in the tumor microenvironment by upregulating PDL1 expression and interacting with PD1 receptors on the surface of immune cells, particularly T cells.[178] Several studies have exploited PDL1 overexpression for tumor imaging and medication targeting. Several antibodies and peptides have been investigated to inhibit the PD1/PDL1 interaction and stimulate tumor-specific T cells.[179,180] Hasanpoor et al[154] prepared human serum albumin-CUR nanoparticles (HSA/Cur NPs) and then functionalized them with PDL1-binding peptide. PDL1-binding peptide was used for targeted delivery of CUR to BC cells with high PDL1 expression. Peptide-HSA/Cur NPs had an average particle size of 246.5 ± 2.5 nm, a PDI of 0.09 ± 0.004, a zeta potential of −24.5 ± 1.5 mV, and EE and DL values of 77.8% and 5.52%, respectively. Peptide-HSA/Cur NPs were found to be more efficiently internalized by high PDL1-expressing cancer cells than HSA/Cur NPs when cellular uptake was evaluated. In high PDL1-expressing BC cells, peptide binding to HSA/Cur NPs greatly boosted cytotoxicity, according to cell viability and apoptosis studies. These findings imply that PDL1 is a good target for the delivery of selective drugs and a therapeutic option for BC cells that express PDL1.

Folic Acid Receptor

The folic acid (FA) receptor is a single-chain membrane glycoprotein receptor that has a high affinity for binding and translocating FA into cells.[181] Because of its low cost and ease of customization, FA has become one of the most extensively approved cancer targeting agents. FA receptors are overexpressed in a range of cancer cells, including breast, colon, and lung cancers.[182] Furthermore, these FA receptors are suitable targeting agents because they are expressed at low levels in normal tissue. FA receptors can therefore be a useful tool for actively targeting different drug delivery systems.[183] Lin et al[155] prepared CUR-loaded lipid nanoparticles (CUR-NLCs). The particle size of FA-CUR-NLC was 126.8 ± 3.4 nm, the PDI was 0.16 ± 0.04, the zeta potential was +12.6 ± 1.8 mV, and the EE and DL were 82.7 ± 2.9 and 5.1 ± 0.8%, respectively. The in vitro results showed that FA-CUR-NLC significantly inhibited the growth of MCF-7 cells. FA-CUR-NLCs also showed better antitumor activity in vivo than other agents. Furthermore, Boroujeni et al[156] developed novel and inexpensive CUR-loaded chitosan nanoparticles for FA targeting. The best formulated nanoparticles had a particle size of 197 ± 20 nm, a zeta potential of −6.55 mV, an EE of 92.06 ± 2.17% and a DL of 4.40 ± 0.10%. Cell viability studies confirmed the good potential of CUR-loaded NPs as a drug delivery system for BC therapy. In addition, Pal et al[157] prepared gum acacia (GA) microspheres loaded with CUR and coupled with FA. The prepared microspheres had a particle size of 813.3 nm, a PDI of 0.341 and a zeta potential of −7.6 mV. The toxicity of the microspheres was evaluated on a TNBC cell line. They were found to induce apoptosis by disrupting the mitochondrial membrane potential. In vivo studies in a BALB/C mouse model showed more tumor regression in the presence of folic acid-targeted CUR-encapsulated GA microspheres.

Transferrin Receptor (TfR)

Transferrin is a serum glycoprotein that interacts with the cell surface transferrin receptor (TfR) to transport iron through the bloodstream and into the cell through receptor-mediated endocytosis.[184] TfR is highly increased on metastatic and drug-resistant malignant tumor cells (up to 100-fold higher than in normal cells), making transferrin and transferrin mimetics attractive for cancer therapeutic delivery.[185] Furthermore, TfR is also expressed on the endothelial cells of brain capillaries. The blood–brain barrier may impede the successful delivery of chemotherapeutic medicines, making TfR an intriguing target for the delivery of chemotherapeutic medications to malignancies beyond the blood–brain barrier.[186] Cui et al[158] designed transferrin-modified nanoparticles (Tf-PEG-CUR/DOX NPs) to codeliver CUR and DOX for BC treatment. The nanoparticles had a particle size of 88.7 ± 3.9 nm, a PDI of 0.14 ± 0.03, and a zeta potential of−15.6 ± 1.6

mV. The EE of CUR and DOX were 85.3 ± 3.2 % and 82.7 ± 4.1 %, respectively, and the CUR DL was 4.6 ± 0.8 %. MCF-7 cells and mice injected with MCF-7 cells were used for in vitro cytotoxicity tests and in vivo antitumor activity tests, respectively. The system showed significantly higher efficiency than the other systems both in vitro and in vivo. When compared to Tf-PEG-CUR NPs, in vitro cell viability tests revealed that the dual-loaded system was more cytotoxic. It was shown that this coencapsulation strategy produced efficient tumor-targeted drug delivery, minimized cytotoxic effects, and showed increased anticancer effects using a mouse transplantation tumor model of BC.

Physicochemical Targeted Drug Delivery System

Recent preclinical animal research has shown promising results with targeted medications based on nanotechnology. Inactivation of numerous targeting ligands, tumor heterogeneity, hypoxia, endosomal escape, and difficulties in controlling drug release from nanocarriers are a few of the current issues confronting drug delivery systems that rely on EPR effects and ligand recognition.[187] Thus, it is helpful for the targeted treatment of cancers if drug delivery systems are developed on the basis of the tumor microenvironment to imitate biological responsiveness and achieve on-demand reaction release of medications. These drug delivery systems are also known as physicochemical TDDSs because they can release drugs in response to particular physical or chemical conditions.[188] To deliver targeted drugs, current physicochemical TDDSs for CUR mostly depend on the chemical endogenous stimuli (pH) and exogenous physical stimuli (temperature, light, and magnetism) of the tumor microenvironment. The physicochemical TDDS of CUR are summarized in Table 4.

pH-Sensitive-Based CUR Delivery

In many cases, medication release into specific organs (eg, the gastrointestinal system or the vagina) or intracellular compartments (eg, endonucleosomes or lysosomes) is triggered by pH changes associated with pathological diseases such as cancer or inflammation.[199] The pH of normal human tissues is approximately 7.4, whereas cancer cells have a high rate of glycolysis under aerobic or anaerobic conditions. A tumor's microenvironment has an acidic pH of 6.0 to 7.2 as a result of glycolysis, and the endosomes and lysosomes of tumor cells have a lower pH of 4.0 to 6.0.[200] The pH difference between tumor tissue and healthy tissue has been utilized by numerous anticancer drug delivery systems with pH-responsive release to enable targeted drug release in tumor tissue. Rashidzadeh et al[189] developed novel polymer-CUR couples (PDCs) based on glycidyl azide polymers (GAPs) for tumor therapy. Since CUR readily couples to amine-containing polymer carriers via imine bonds and the coupling remains stable under normal physiological conditions while readily dissociating in acidic environments, the release of CUR at tumor tissues achieves tumor growth inhibition. The results showed that the prepared PDCs self-assembled in aqueous solution to form nanomicelles with an average particle size of 180 nm and good polydispersity. The drug release study showed that the PDC micelles were quite stable in the physiological environment, but a mildly acidic environment triggered the release of CUR. The PDC micelles showed a good cytotoxic effect on a mouse BC cell line (4T1 cells), while the unloaded micelles had no significant toxic effect on tumor cells. Moreover, Ji et al[190] constructed a pH-sensitive tumor self-targeted drug delivery system (CUR@HFn) by wrapping CUR in recombinant human heavy chain apoferritin (HFn) cavities using a self-assembly technique (Figure 10). The results show that CUR@HFn has a hydrodynamic diameter of 19.6 nm, a PDI of 0.272 and a zeta potential of −10.8 mV. CUR@HFn was pH-sensitive and displayed sustained drug release under slightly acidic conditions, according to in vitro release assays. CUR@HFn demonstrated more cytotoxicity, cellular uptake, and targeting than CUR. In addition, Ghaffari et al[191] synthesized N-succinyl chitosan-functionalized ZnO nanoparticles as a pH-sensitive drug delivery system (CUR-CS-ZnO) to enhance the therapeutic potential of CUR. The results showed that the concentration of CUR in the formulation was approximately 130 μg/mg of the complex. The coupling efficiency was 69.6%, and the hydrodynamic diameter of CUR-CS-ZnO was approximately 130 nm. The in vitro release results showed that the cumulative release of CUR from CUR-CS-ZnO was significantly higher in a low pH environment, which allowed the drug to be delivered to the tumor site for therapeutic effects. Cellular assay results showed that CUR-CS-ZnO had better anticancer activity against BC cells (MDA-MB-231 cells) than free CUR.

Table 4 Physicochemically TDDS for CUR

Drug Delivery System	Stimulus-Response Properties	Efficacy	Ref., Year
GAP-CUR conjugates	pH sensitivity: cumulative release of CUR: pH = 5.6 > pH = 7.4	4T1 cells (48/72 h, CUR: IC_{50} = 19/15 μg/mL, PDCs: IC_{50} = 10/7 μg/mL)	2021[189]
CUR loaded HFn	pH sensitivity: cumulative release of CUR: pH = 5 > pH = 6 > pH = 7.4	Cellular uptake (4T1 cells ↑); 4T1/MDA-MB-231 cells viability (CUR@HFn < CUR); 4T1 cells (cell apoptosis: CUR = 8.25%, CUR@HFn = 14.39%); 4T1 tumor inhibition rate: (CUR@HFn (20 mg/kg, *iv*., once every two days for 12 days) > CUR (20 mg/kg, *iv*., once every two days for 12 days))	2022[190]
CUR-CS-ZnO nanoparticles	pH sensitivity: cumulative release of CUR: pH = 5.2 > pH = 7.4	MDA-MB-231 cells (48 h, CUR: IC_{50} = 5 μg/mL, CUR-CS-ZnO: IC_{50} = 40.1 μg/mL, cell apoptosis: CUR (3/5 μg/mL) = 24.46/44.83%, CUR-CS-ZnO (3/5 μg/mL) =90.3/97.2%)	2020[191]
Fe_3O_4-CRC-TRC-NPs	Thermosensitive: cumulative release of CUR: Fe_3O_4-CRC-TRC-NPs (RF 80 W/2 min)> Fe_3O_4-CRC-TRC-NPs (NO RF)	4T1 cells viability (Fe_3O_4-CRC-TRC-NPs (NO RF) > Fe_3O_4-CRC-TRC-NPs (RF 80 W/2 min)); 4T1 cells (cell apoptosis: Fe_3O_4-CRC-TRC-NPs (NO RF) = 43.3%, Fe_3O_4-CRC-TRC-NPs (RF 80 W/2 min) = 96.1%); Ex-vivo optical imaging (*iv*.): tumor ↑	2016[192]
CUR-loaded thermosensitive microgels	Thermosensitive	MDA-MB-231 cells (24 h, CUR: IC_{50} = (2.5 ± 0.6) μg/mL, microgels: IC_{50} = (3.8 ± 0.2) μg/mL)	2021[193]
CUR-loaded thermosensitive nanogels	Thermosensitive: cumulative release of CUR: AuNP@Ng/CUR (37 °C) > AuNP@Ng/CUR (25 °C)	Cellular uptake (MDA-MB-231 cells ↑); MDA-MB-231 cells viability (AuNP@Ng/CUR (NO laser) > AuNP@Ng/CUR (laser))	2020[194]
Photosensitive carrier-free CUR nanodrugs (CUR NDs)	Light responsiveness: CUR ND drug release rate in the presence of radiation becomes much faster than in the absence of radiation.	Cellular uptake (4T1 cells (after light irradiation) ↑); 4T1 cells (24 h, CUR: IC_{50} = (23.61 ± 0.16) μg/mL, CUR NDs: IC_{50} = (13.74 ± 0.13) μg/mL, CUR (Light: 450 nm/640 mW/1 min): IC_{50} = (19.38 ± 0.15) μg/mL, CUR NDs (Light: 450 nm/640 mW/1 min): IC_{50} = (5.36 ± 0.14) μg/mL, cell apoptosis: CUR = (8.08 ± 0.42) %, CUR NDs = (21.08 ± 2.14) %, CUR (Light: 450 nm/640 mW/1 min) = (15.38 ± 1.73) %, CUR NDs (Light: 450 nm/640 mW/1 min) = (32.22 ± 1.99) %); 4T1 cells (P-JNK, Bax, Cleaved caspase 3 ↑)	2019[195]
CUR-loaded layered double hydroxide nanohybrid (CUR-LDH nanohybrid)	Light responsiveness	MDA-MB-231 cells lactate dehydrogenase release (24 h, CUR-LDH nanohybrid (465 nm; power density: 34 mW/cm^2) > CUR-LDH nanohybrid (non-irradiated); MDA-MB-231 cells (cell apoptosis: CUR-LDH nanohybrid (465 nm; power density: 34 mW/cm^2) (25/100 μg/mL) = 22.54/34%)	2019[196]
CUR loaded amino acids modified iron oxide magnetic nanoparticles (F@AAs@CUR NPs)	Magnetic	HFF-2 and HEK 293 cells (F@AAs@CUR NPs (No toxic effect)); MCF7 cells viability (40–80 μM, F@Lys@CUR NP and F@PhA@CUR NP > CUR)	2018[197]

(*Continued*)

https://doi.org/10.2147/IJN.S410688 DovePress

Table 4 (Continued).

Drug Delivery System	Stimulus-Response Properties	Efficacy	Ref., Year
Co-loaded letrozole and CUR magnetic vesicle nanocarriers ($NiCoFe_2O_4$ @L-Silica@C-Niosome)	Magnetic	MCF-10A cells (72 h, CUR: IC_{50} = 561.51 μg/mL, letrozole: IC_{50} = 587.27 μg/mL, CUR + letrozole: IC_{50} = 401.3 μg/ mL, $NiCoFe_2O_4$@L-Silica@C-Niosome: IC_{50} = 842.2 μg/ mL); SK-BR-3 cells (48 h, CUR: IC_{50} = 431.62 μg/mL, letrozole: IC_{50} = 337.82 μg/mL, $NiCoFe_2O_4$@L-Silica@C-Niosome: IC_{50} = 39.48 μg/mL, cell apoptosis: CUR = (13.13 ± 1.45) %, letrozole = (10.94 ± 0.80) %, CUR + letrozole = (17.32 ± 0.69) %, $NiCoFe_2O_4$@L-Silica@C-Niosome = (48.63 ± 1.94) %); MDA-MB-231 cells (48 h, CUR: IC_{50} = 414.15 μg/mL, letrozole: IC_{50} = 354.81 μg/mL, $NiCoFe_2O_4$@L-Silica@C-Niosome: IC_{50} = 93.47 μg/mL, cell apoptosis: CUR = (9.43 ± 0.46) %, letrozole = (7.10 ± 1.82) %, CUR + letrozole = 15.54 ± 2.33%, $NiCoFe_2O_4$ @L-Silica@C-Niosome = (37.70 ± 2.26) %); SK-BR-3 and MDA-MB-231 cells (Bax, Caspase 3, Caspase 9 ↑, Bcl 2, Cyclin D, Cyclin E, MMP-2, MMP-9 ↓); SK-BR-3 and MDA-MB-231 cells (Migration rate ↓)	2021[198]

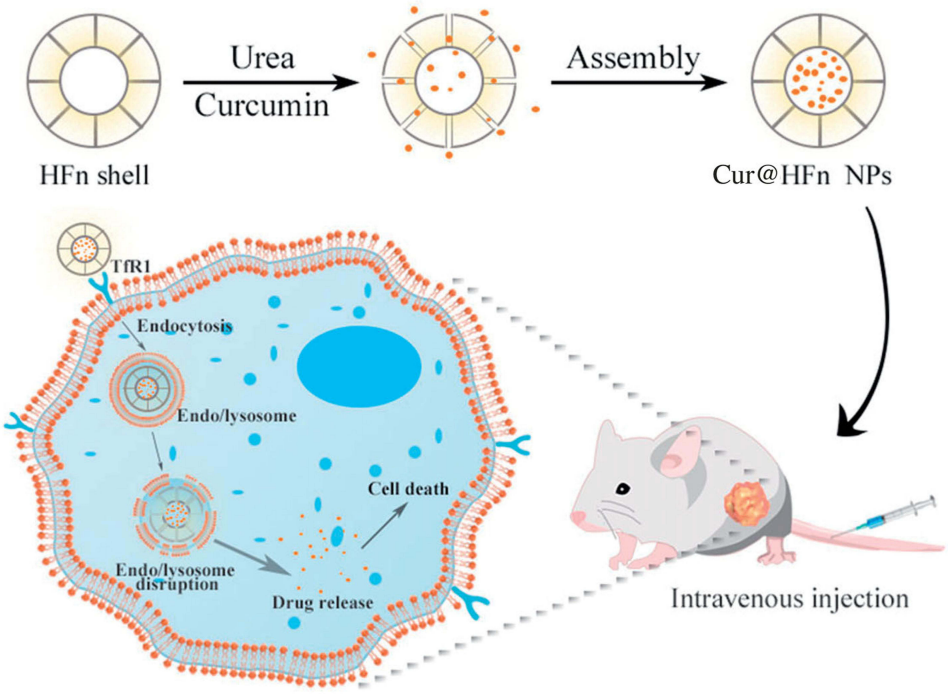

Figure 10 Schematic illustration of Cur@HFn for anticancer therapy. Reproduced with permission from Ji P, Wang X, Yin J, et al. Selective delivery of curcumin to breast cancer cells by self-targeting apoferritin nanocages with pH-responsive and low toxicity. *Drug Deliv.* 2022;29(1):986–996. Creative Commons.[190]

Thermoresponsive-Based CUR Delivery

Thermoresponsive release is among the most researched methods for delivering smart drugs is thermoresponsive release because it can take advantage of local temperature rises caused by disease (eg, tumors, inflammation, or infection).[201] Thermoresponsive release is based on dramatic alteration of the physical properties of temperature-sensitive materials. When there is a change in temperature close to the carrier, this rapid response can cause the medicine to be released.[202] Rejinold et al[192] used noninvasive radiofrequency (RF) frequencies as an energy source to activate Fe_3O_4-embedded thermosensitive nanoparticles (Fe_3O_4-CRC-TRC-NPs) for targeted delivery of CUR to BC cells with therapeutic efficacy. The prepared Fe_3O_4-CRC-TRC-NPs had a particle size of 170 ± 24 nm and a zeta potential of 22.76 ± 1.8 mV. Treatment of Fe_3O_4-CRC-TRC-NPs with 80-watt RF for 2 min thermogenically reached 42 °C and induced controlled CUR release and apoptosis in cultured 4T1 cells. In addition, tumor localization studies on in situ BC models revealed selective accumulation of Fe_3O_4-CRC-TRC-NPs at the primary tumor, which was confirmed by in vivo live imaging, ex vivo tissue imaging and HPLC studies. Kulkarni et al[193] developed microgels loaded with CUR based on Pluronic F-127. The hydrodynamic diameter of the microgels was approximately 544 nm, and the DL was approximately 40%. In vitro release results showed that the microgels exhibited pH- and temperature-dependent release, with the fastest release rate of CUR at 45 °C and a slow and sustained release of CUR at 37 °C and under acidic conditions. In vitro cytotoxicity results performed on MDA-MB-231 cells showed that the microgels and CUR showed comparable effects on cancer cells. In addition, Howaili et al[194] synthesized plasma nanogels (AuNP@Ng/CUR) with dual temperature-pH responsiveness by grafting poly-N-isopropylacrylamide (PNIPAM) onto chitosan in the presence of a chemical cross-linker, which was used as a CUR carrier and further combined with gold nanoparticles to provide simultaneous drug delivery and photothermal therapy. AuNP@Ng/CUR had a hydrodynamic size of 226 ± 1.49 nm, a PDI of 0.354, a zeta potential of 0.676 mV, and CUR EE and DL of 92 ± 0.98% and 17.01 ± 0.33%, respectively. To examine the photothermal activity of AuNP@Ng/CUR, the thermal analysis of AuNP@Ng/CUR after exposure to an 808 nm near-infrared (NIR) laser was evaluated at different points in time. The results

showed that the temperature of AuNP@Ng/CUR increased by 5.1 °C compared to the control. The prepared nanoparticles showed better in vitro therapeutic effects under NIR laser (808 nm) irradiation.

Light-Based CUR Delivery

Due to its remote controllability and potential for high spatial and temporal resolution, the use of light as a stimulus to promote drug release has drawn considerable interest in tumor therapy.[203] This treatment is also called photodynamic therapy (PDT). PDT is carried out by providing a photosensitizer (Ps) followed by irradiation with light at the precise wavelength of maximum absorption of Ps. In the presence of tissue oxygen, Ps molecules undergo electronic changes that lead to the direct or indirect death of tumor cells by the generation of reactive oxygen species (ROS) and free radicals.[204,205] Sun et al[195] prepared carrier-free CUR nanodrugs (CUR NDs) by a simple, green reprecipitation method without the use of any toxic solvents. CUR NDs had a hydrodynamic diameter of approximately 74.56 nm and a zeta potential of −23.14 mV. CUR NDs had unique optical properties and photosensitive drug release behavior, and compared to free CUR, the ROS production was increased and the PDT effect on BC cells was enhanced. Under light irradiation, CUR ND resulted in a significant decrease in 4T1 cell survival compared to free CUR. The study suggests that CUR NDs are an effective nanodrug for PDT in BC and show considerable clinical translational potential. Moreover, Khorsandi et al[196] prepared a layered double hydroxide nanohybrid (CUR-LDH nanohybrid) loaded with CUR. The particle size of the CUR-LDH nanohybrid ranged from 70–90 nm. Cellular assays showed that CUR-LDH nanohybrid with irradiation had cytotoxic and proliferation inhibitory effects on MDA-MB-231 cells. CUR-LDH nanohybrid with irradiation induced autophagy, apoptosis and G0/G1 cell cycle arrest in human BC cell lines. Intracellular ROS were increased in MDA-MB-231 cancer cell lines after treatment with the CUR-LDH nanohybrid along with irradiation.

Magnetism-Based CUR Delivery

Magnetic nanoparticles (MMPs) have the advantages of low toxicity, small size, easy preparation and low production cost and have great potential for medical applications due to their unique physicochemical properties, especially as carriers for TDDS.[206] A natural amino acid modified iron oxide magnetic nanoparticle loaded with CUR was prepared by Nosrati et al.[197] Two amino acids, L-lysine (Lys) and L-phenylalanine (PhA), were selected to modify the nanoparticles, and their effects on CUR loading, release characteristics, biocompatibility and anticancer activity were investigated. The particle sizes of the two nanoparticles, F@Lys@CUR NP and F@PhA@CUR NP, were 20.20 ± 2.51 nm and 23.11 ± 4.56 nm, respectively, with zeta potentials of −15.7 and −6.45 mV, respectively. The DL in F@Lys@CUR NP and F@PhA@CUR NP were 3.44% and 4.39%, respectively. The results of nanoparticle magnetization studies showed a decrease in the saturation magnetization intensity of F@Lys@CUR NP and F@PhA@CUR NP. The in vitro release results showed that the DL of F@PhA@CUR NPs was greater than that of F@Lys@CUR NPs, but the release rate of F@Lys@CUR NPs was greater than that of F@PhA@CUR NPs. The results of in vitro antitumor studies showed that the anticancer activity of F@PhA@CUR NPs and F@Lys@CUR NPs in the CUR concentration range of 40–80 μM was lower than that of free CUR. In addition, Jamshidifar et al[198] coated the magnetic $NiCoFe_2O_4$ core with a thin layer of silica followed by a liposomal structure, loaded letrozole and CUR into the silica and liposomal layers, respectively, and studied their synergistic effects on BC cells. The average hydrodynamic diameter of the prepared dual-loaded nanoparticles ($NiCoFe_2O_4$@L-Silica@C-Niosome) was 138.7 nm with a PDI of 0.236. The EEs of CUR and letrozole in the $NiCoFe_2O_4$@L-Silica@C-Niosome were 81.21% and 92.73%, respectively. The study of the super magnetic properties of $NiCoFe_2O_4$ and $NiCoFe_2O_4$@Silica nanoparticles showed that the magnetic properties of $NiCoFe_2O_4$ nanoparticles were 17.58 emu/g, while the magnetic properties of $NiCoFe_2O_4$@Silica (11.71 emu/g) were slightly weaker than those of $NiCoFe_2O_4$ nanoparticles. The results of cellular assays showed that $NiCoFe_2O_4$@L-Silica@C-Niosome had a stronger inhibitory effect on cancer cells and triggered more apoptosis of tumor cells. Finally, $NiCoFe_2O_4$ @L-Silica@C-Niosome also significantly reduced the migration level of BC cells.

New Developments in CUR Drug Delivery Systems

Exosomes are extracellular microvesicles that can shuttle in and out of cells and carry large amounts of proteins, lipids, RNA, and DNA. Because of their ability to do so, these particles may be employed as nanodrug carriers. Exosomes have the advantages of good biocompatibility, high stability in blood, low immunoantigenicity, and natural targeting

ability.[207–209] Aqil et al[108] demonstrated that CUR can be efficiently delivered using milk-derived exosomes. In the presence of 10% ethanol: acetonitrile (1: 1), CUR loading in exosomes can reach 18–24%. Cancer cells ingest exosomes through caveolae/clathrin-mediated endocytosis. ExoCUR levels in several organs were 3–5 times higher in Sprague–Dawley rats after oral administration compared to free drug. In comparison to free CUR, ExoCUR demonstrated improved antiproliferative efficacy against several cancer cell lines, including breast, lung, and cervical cancers. In addition, González-Sarrías et al[109] loaded CUR and resveratrol (RSV) into breast-derived exosomes (EXO-CUR and EXO-RSV, respectively) and compared their delivery capacity to breast tissue and their anticancer activity. The results showed that CUR and RSV peaked in breast tissue 6 min after intravenous injection of EXO-CUR and EXO-RSV (41 ± 15) and (300 ± 80) μM, respectively. EXO-CUR or EXO-RSV exerted effective antiproliferative effects on cancer cells but had no effect on normal cells. Milk EXOs served as a Trojan horse to circumvent'ABC-mediated chemoresistance in cancer cells, which increased the bioavailability and anticancer activity of CUR and RSV.

Colloidal systems made up of oily cores encased in a polymeric shell are called liquid lipid nanocapsules (LLNs). Due to their hydrophobicity, they can achieve high EE,[210] and due to their polymeric shell, they can reduce tissue irritation at the deposition site.[211] González et al[110] prepared an LLN covered with human serum albumin (HSA) protein and loaded with CUR and measured the diameter of the LLN to be 169 ± 4 nm and the PDI to be 0.19 ± 0.05. Cellular uptake and killing ability were evaluated on the human BC cell line MCF-7, and the results showed that LLN exhibited similar half maximum inhibitory concentration (IC_{50}) capacity as free CUR and showed excellent uptake performance with massive cell entry in less than 1 min.

Materials based on graphene have become increasingly interesting to researchers working in the field of nanobiotechnology in recent years.[212,213] The immune system can be stimulated by graphene, activating macrophages. In addition, high levels of graphene can cause macrophages to undergo apoptosis and immune-suppressive reactions.[214] Due to its large surface area to volume ratio and unique chemical and physical properties, graphene oxide (GO) exhibits antibacterial, antifungal, and antiviral capabilities. To achieve synergistic benefits, graphene-based materials combined with medications have been developed for cancer therapy.[215] De et al[111] prepared GO and graphene quantum dots (GQDs) with CUR in three different ratios (1:1, 1:3 and 1:5 w/v). UV–Vis estimated DL of 80 ± 1 % and 83 ± 1 % for GO-CUR and GQDs-CUR, respectively. The cytotoxic effects of different ratios of GO-CUR and GQDs-CUR as anticancer drugs on human BC cell lines MCF-7 and MDA-MB-468 were tested by MTT assay. The results showed that for both cell lines with a 1:5 ratio of GO-CUR and GQDs-CUR, cell death exceeded 90%, even at very low concentrations of the complexes (10–20 μg/mL). In all concentration ranges, the complexes demonstrated a higher rate of cell killing than free CUR. In comparison to GO-CUR, GQDs-CUR performed better in both BC cell lines.

Conclusions

BC, one of the most common cancers, is a constant threat to human health. The survival rate of BC patients, especially in developing countries, is less than 40%. Common treatments for BC include hormonal therapy, surgery, targeted therapy, radiation therapy and chemotherapy. Approximately 70% of all BCs can be classified as ER positive and can be treated with antiestrogenic drugs such as raloxifene or tamoxifen. However, the use of single molecules is not particularly effective in treatment, and a number of factors, such as side effects during treatment and poor surgical healing, have motivated researchers to seek an alternative treatment. The use of natural drugs to treat BC is considered to be a promising approach, as natural drugs have the advantage of being less toxic and having fewer side effects than chemical drugs. Today, an increasing number of cancer patients are already using natural drugs as a supplement and alternative to conventional drugs. Among various natural drugs, CUR has received much attention for its broad range of anticancer activities, and CUR is considered to be an effective anticancer agent that regulates a variety of intracellular signaling pathways. Discussions of the anticancer effects of CUR have emerged in recent decades. Sharma et al[216] treated 15 patients with standard chemotherapy-refractory advanced colorectal cancer with CUR for up to 4 months successfully treated colon cancer with CUR in a Phase I clinical trial. Cruz-Correa et al[217] evaluated the efficacy of the combination of CUR and quercetin in the treatment of adenoma regression in patients with familial adenomatous polyposis (FAP) (FAP is a genetic disease that predisposes patients to colon cancer). The combination of CUR and quercetin was found to reduce the number and size of ileal and rectal

adenomas in patients with FAP without significant toxicity. In addition, the results of a Phase II clinical study by Howells et al showed that CUR is a safe and tolerated adjuvant to chemotherapy in patients with metastatic colorectal cancer.[218] Many studies on different cancer treatments (both preclinical and clinical trials) have shown that CUR is a promising anticancer agent that can be used alone or in combination with other drugs.[219–224]

However, CUR's clinical application in BC is constrained by its low bioavailability, poor water solubility, short half-life, fast metabolism, and inadequate tumor targeting capacity. Therefore, researchers have developed different drug delivery systems to address these problems, and great progress has been made in recent years. CUR-loaded drug delivery systems can be divided into three categories according to the type of targeting: passive targeting, active targeting and physicochemical targeting. First, passively TDDSs loaded with CUR include liposomes, micelles, nanogels, nanoparticles (containing SLN, polymer nanoparticles, MSN and gold nanoparticles), nanoemulsions and so on, which significantly improve the bioavailability, solubility, absorption and metabolism of CUR in vivo. The EPR effect enables these drug delivery systems to passively accumulate CUR in tumor tissues, and slow, continuous drug release considerably improves CUR's antitumor activity. Second, active TDDSs loaded with CUR can further enhance the antitumor effect of CUR by modifying specific ligands, such as proteins, antibodies, peptides or small chemical molecules, on the surface of the drug delivery system so that they specifically bind to surface antigens or receptors expressed in tumor tissues, thus triggering endocytosis of tumor cells, achieving targeted drug delivery and reducing the distribution of the drug in normal tissues. In this paper, active TDDSs are classified according to the targeted antigen or receptor into the HER2 receptor, EGFR, CD44, integral protein αvβ3, PDL1, FA receptor and TfR. They all have a common feature in that their expression in tumor tissues is different from that in normal tissues and can bind specifically to TDDSs, thus achieving drug enrichment in tumor tissues. Finally, the physicochemical TDDS loaded with CUR is based on the tumor microenvironment to design a drug release system that mimics biological responsiveness to achieve on-demand drug release, which is beneficial to the precision treatment of tumors. The physicochemical TDDSs loaded with CUR summarized in this paper are mainly divided into chemical endogenous stimulus (pH) response and exogenous physical stimulus (temperature, light and magnetic) response systems, which are important for controlling drug release at the target site.

Considerable research has been conducted on CUR TDDSs, but many challenges remain before these systems can be used in clinical practice. First, for passive TDDSs, drugs are mainly delivered to different parts of the body through normal physiological processes using particles (liposomes, micelles, nanogels, nanoparticles, nanoemulsions, etc.) as carriers, and they demonstrate a certain superiority over free drugs. However, different passive TDDSs have their own drawbacks, such as the low encapsulation rate of liposomes, and the drug can easily leak from the liposomes and thus cannot effectively play its modifying or encapsulating role.[225,226] In addition, poor stability needs to be addressed in the commercialization of liposomes.[227,228] The poor stability of micelles is also an important reason they are difficult to apply. Moreover, the enrichment of micelles is not great, resulting in only moderately pronounced efficacy, which is also a major limitation.[229–231] Nanogels are formed by physical or chemical cross-linking of carrier materials, and each has its own shortcomings depending on its preparation method. Nanogels prepared by physical crosslinking methods have the disadvantage of poor stability because the noncovalent interaction is relatively weak, and when the external conditions change, the nanogel will be destroyed and the drug will be easily released from the nanogel, while nanogels prepared by chemical crosslinking methods have relatively good stability, but chemical substances and surfactants may be introduced during the preparation process, thus creating safety problems.[232,233] Therefore, it is necessary to seek a green and safe synthesis technology. For nanoparticles, problems such as low DL, organic solvent residues during preparation, poor dispersibility and agglomeration are common.[234,235] For nanoemulsions, their poor thermal stability, limited industrial production, low-toxicity and efficient surfactants and cosurfactants still need to be developed, and the preparation process needs to be improved, which are major obstacles to their promotion and application and are also the main factors leading to few varieties on the market.[236,237] Second, active TDDSs can deliver the drug to the target area in a directed and concentrated way to exert the drug effect, which is highly concentrated and therefore has fewer toxic side effects.[238] However, there are some problems in its application, such as its preparation process being generally complex, expensive, and difficult to adapt to industrial production, and when it is truly applied in the clinic, its effect will be different depending on each person's constitution.[239] Finally, for physicochemical TDDSs, certain physicochemical methods can be applied to make the targeted agents effective at specific sites.[240] The main problems facing its development are

that it is expensive, prone to allergic reactions, and its efficacy varies in different individuals due to tumor heterogeneity.[241,242] The current research on physicochemical TDDS is not yet in depth, and more extensive and in-depth research is needed in the future. In conclusion, whether passive, active or physicochemical TDDSs are to be used in clinical practice, safety issues should be considered first, followed by problems faced by industrialization, such as preparation processes and production costs. The advancement of CUR TDDSs to clinical practice depends on the continuous resolution of the above issues.

In the past few years, CUR-TDDSs have demonstrated their therapeutic potential as cancer drugs, and while they have shown promise for cancer diagnosis and precision drug delivery, more research is needed to minimize their toxicity and improve their efficacy. The ideal CUR-TDDS for clinical applications should be able to deliver the drug to the target site in a precise and stable manner with stable controlled drug release, and the delivery vehicle and materials should be nontoxic and biodegradable to maximize efficacy and minimize health risks. Moreover, as nanotechnology research continues, the development of new theories will open up new directions for CUR nanotechnology in the diagnosis and treatment of cancer and other diseases. Based on the existing theories of nanosolubilization, targeted modulation or touch release, the integration of frontier scientific theories with nanotechnology using artificial intelligence, 3D printing, biomedicine and bioinformatics will be an opportunity for nanotechnology to further flourish. Under the guidance of the new theories, nanotechnology will be more energetic, comprehensively improve the clinical treatment effect of various diseases, and further improve the scientific process of human disease diagnosis, prevention and treatment.

Acknowledgments

This research was supported by grants from National Natural Science Foundation of China (grant No. 82204935), Natural Science Basic Research Program Project of Shaanxi Province (grant No. 2022JQ-917), Key Scientific Research Project of Shaanxi Provincial Department of Education (grant No. 21JS009), School-level Scientific Research Project of Shaanxi University of Traditional Chinese Medicine (grant No. 2021GP04), Key Scientific Research Project of Shaanxi Provincial Department of Education (grant No. 21JS014).

Disclosure

The authors declare that they have no known competing financial interests or personal relationships that could have appeared to influence the work reported in this paper.

References

1. Akram M, Iqbal M, Daniyal M, Khan AU. Awareness and current knowledge of breast cancer. *Biol Res*. 2017;50:33. doi:10.1186/s40659-017-0140-9
2. Merino Bonilla JA, Torres Tabanera M, Ros Mendoza LH. Breast cancer in the 21st century: from early detection to new therapies. *Radiologia*. 2017;59:368–379. doi:10.1016/j.rx.2017.06.003
3. Ren W, Chen M, Qiao Y, Zhao F. Global guidelines for breast cancer screening: a systematic review. *Breast*. 2022;64:85–99. doi:10.1016/j.breast.2022.04.003
4. Subik K, Lee J-F, Baxter L, et al. The expression patterns of ER, PR, HER2, CK5/6, EGFR, Ki-67 and AR by immunohistochemical analysis in breast cancer cell lines. *Breast Cancer*. 2010;4:35–41.
5. Mota ADL, Evangelista AF, Macedo T, et al. Molecular characterization of breast cancer cell lines by clinical immunohistochemical markers. *Oncol Lett*. 2017;13(6):4708–4712. doi:10.3892/ol.2017.6093
6. Nolan E, Lindeman GJ, Visvader JE. Deciphering breast cancer: from biology to the clinic. *Cell*. 2023;186(8):1708–1728. doi:10.1016/j.cell.2023.01.040
7. Li Y, Zhang H, Merkher Y, et al. Recent advances in therapeutic strategies for triple-negative breast cancer. *J Hematol Oncol*. 2022;15(1):121. doi:10.1186/s13045-022-01341-0
8. Yallapu MM, Jaggi M, Chauhan SC. Curcumin nanomedicine: a road to cancer therapeutics. *Curr Pharm Des*. 2013;19:1994–2010. doi:10.2174/138161213805289219
9. Yadav N, Parveen S, Banerjee M. Potential of nano-phytochemicals in cervical cancer therapy. *Clin Chim Acta*. 2020;505:60–72. doi:10.1016/j.cca.2020.01.035
10. Pradhan D, Biswasroy P, Sahu A, et al. Recent advances in herbal nanomedicines for cancer treatment. *Curr Mol Pharmacol*. 2021;14(3):292–305. doi:10.2174/1874467213666200525010624
11. Rauf A, Imran M, Butt MS, et al. Resveratrol as an anti-cancer agent: a review. *Crit Rev Food Sci Nutr*. 2018;58(9):1428–1447. doi:10.1080/10408398.2016.1263597
12. Mirahmadi M, Azimi-Hashemi S, Saburi E, et al. Potential inhibitory effect of lycopene on prostate cancer. *Biomed Pharmacother*. 2020;129:110459. doi:10.1016/j.biopha.2020.110459
13. Bailly C. Irinotecan: 25 years of cancer treatment. *Pharmacol Res*. 2019;148:104398. doi:10.1016/j.phrs.2019.104398

14. Albalawi AE, Alanazi AD, Sharifi I, Ezzatkhah F. A systematic review of curcumin and its derivatives as valuable sources of antileishmanial agents. *Acta Parasitol*. 2021;66(3):797–811. doi:10.1007/s11686-021-00351-1
15. Mahmoudvand H, Pakravanan M, Aflatoonian MR, et al. Efficacy and safety of Curcuma longa essential oil to inactivate hydatid cyst protoscoleces. *BMC Complement Altern Med*. 2019;19:187. doi:10.1186/s12906-019-2527-3
16. Naksuriya O, Okonogi S, Schiffelers RM, Hennink WE. Curcumin nanoformulations: a review of pharmaceutical properties and preclinical studies and clinical data related to cancer treatment. *Biomaterials*. 2014;35(10):3365–3383. doi:10.1016/j.biomaterials.2013.12.090
17. Rashwan AK, Karim N, Xu Y, et al. An updated and comprehensive review on the potential health effects of curcumin-encapsulated micro/nanoparticles. *Crit Rev Food Sci Nutr*. 2022:1–21. doi:10.1080/10408398.2022.2070906
18. Pooresmaeil M, Namazi H. Facile preparation of pH-sensitive chitosan microspheres for delivery of curcumin; characterization, drug release kinetics and evaluation of anticancer activity. *Int J Biol Macromol*. 2020;162:501–511. doi:10.1016/j.ijbiomac.2020.06.183
19. Fang Z, Pan S, Gao P, et al. Stimuli-responsive charge-reversal nano drug delivery system: the promising targeted carriers for tumor therapy. *Int J Pharm*. 2020;575:118841. doi:10.1016/j.ijpharm.2019.118841
20. Kumari P, Ghosh B, Biswas S. Nanocarriers for cancer-targeted drug delivery. *J Drug Target*. 2016;24(3):179–191. doi:10.3109/1061186x.2015.1051049
21. Li B, Shao H, Gao L, et al. Nano-drug co-delivery system of natural active ingredients and chemotherapy drugs for cancer treatment: a review. *Drug Deliv*. 2022;29(1):2130–2161. doi:10.1080/10717544.2022.2094498
22. Raj S, Khurana S, Choudhari R, et al. Specific targeting cancer cells with nanoparticles and drug delivery in cancer therapy. *Semin Cancer Biol*. 2021;69:166–177. doi:10.1016/j.semcancer.2019.11.002
23. Zhang G, Zeng X, Li P. Nanomaterials in cancer-therapy drug delivery system. *J Biomed Nanotechnol*. 2013;9(5):741–750. doi:10.1166/jbn.2013.1583
24. Cisterna BA, Kamaly N, Choi WI, et al. Targeted nanoparticles for colorectal cancer. *Nanomedicine*. 2016;11(18):2443–2456. doi:10.2217/nnm-2016-0194
25. Ahmad A, Khan F, Mishra RK, Khan R. Precision cancer nanotherapy: evolving role of multifunctional nanoparticles for cancer active targeting. *J Med Chem*. 2019;62(23):10475–10496. doi:10.1021/acs.jmedchem.9b00511
26. Alavi M, Hamidi M. Passive and active targeting in cancer therapy by liposomes and lipid nanoparticles. *Drug Metab Pers Ther*. 2019;34(1). doi:10.1515/dmpt-2018-0032
27. Janjua KA, Shehzad A, Shahzad R, Islam SU, Islam MU. Nanocurcumin: a double-edged sword for microcancers. *Curr Pharm Des*. 2020;26(45):5783–5792. doi:10.2174/1381612826666201118100045
28. Hussain Y, Islam L, Khan H, et al. Curcumin–cisplatin chemotherapy: a novel strategy in promoting chemotherapy efficacy and reducing side effects. *Phytother Res*. 2021;35(12):6514–6529. doi:10.1002/ptr.7225
29. Kabir MT, Rahman MH, Akter R, et al. Potential role of curcumin and its nanoformulations to treat various types of cancers. *Biomolecules*. 2021;11(3):392. doi:10.3390/biom11030392
30. Maleki Dizaj S, Alipour M, Dalir Abdolahinia E, et al. Curcumin nanoformulations: beneficial nanomedicine against cancer. *Phytother Res*. 2022;36(3):1156–1181. doi:10.1002/ptr.7389
31. Mahmoudi A, Kesharwani P, Majeed M, Teng Y, Sahebkar A. Recent advances in nanogold as a promising nanocarrier for curcumin delivery. *Colloids Surf B Biointerfaces*. 2022;215:112481. doi:10.1016/j.colsurfb.2022.112481
32. Priyadarsini KI. The chemistry of curcumin: from extraction to therapeutic agent. *Molecules*. 2014;19(12):20091–20112. doi:10.3390/molecules191220091
33. Tomeh MA, Hadianamrei R, Zhao X. A review of curcumin and its derivatives as anticancer agents. *Int J Mol Sci*. 2019;20(5):1033. doi:10.3390/ijms20051033
34. Strimpakos AS, Sharma RA. Curcumin: preventive and therapeutic properties in laboratory studies and clinical trials. *Antioxid Redox Signal*. 2008;10(3):511–545. doi:10.1089/ars.2007.1769
35. Kotha RR, Luthria DL. Curcumin: biological, pharmaceutical, nutraceutical, and analytical aspects. *Molecules*. 2019;24(16):2930. doi:10.3390/molecules24162930
36. Heger M, van Golen RF, Broekgaarden M, Michel MC. The molecular basis for the pharmacokinetics and pharmacodynamics of curcumin and its metabolites in relation to cancer. *Pharmacol Rev*. 2014;66(1):222–307. doi:10.1124/pr.110.004044
37. Payton F, Sandusky P, Alworth WL. NMR study of the solution structure of curcumin. *J Nat Prod*. 2007;70(2):143–146. doi:10.1021/np060263s
38. Nelson KM, Dahlin JL, Bisson J, et al. The essential medicinal chemistry of curcumin. *J Med Chem*. 2017;60(5):1620–1637. doi:10.1021/acs.jmedchem.6b00975
39. Mari M, Carrozza D, Ferrari E, Asti M. Applications of radiolabelled curcumin and its derivatives in medicinal chemistry. *Int J Mol Sci*. 2021;22(14):7410. doi:10.3390/ijms22147410
40. Schneider C, Gordon ON, Edwards RL, Luis PB. Degradation of curcumin: from mechanism to biological implications. *J Agric Food Chem*. 2015;63(35):7606–7614. doi:10.1021/acs.jafc.5b00244
41. Feng T, Wei Y, Lee RJ, Zhao L. Liposomal curcumin and its application in cancer. *Int J Nanomedicine*. 2017;12:6027–6044. doi:10.2147/ijn.S132434
42. Zhai B, Zeng Y, Zeng Z, et al. Drug delivery systems for elemene, its main active ingredient β-elemene, and its derivatives in cancer therapy. *Int J Nanomedicine*. 2018;13:6279–6296. doi:10.2147/ijn.S174527
43. Rein MJ, Renouf M, Cruz-Hernandez C, et al. Bioavailability of bioactive food compounds: a challenging journey to bioefficacy. *Br J Clin Pharmacol*. 2013;75(3):588–602. doi:10.1111/j.1365-2125.2012.04425.x
44. Dei Cas M, Ghidoni R. Dietary curcumin: correlation between bioavailability and health potential. *Nutrients*. 2019;11(9):2147. doi:10.3390/nu11092147
45. Lopresti AL. The problem of curcumin and its bioavailability: could its gastrointestinal influence contribute to its overall health-enhancing effects? *Adv Nutr*. 2018;9(1):41–50. doi:10.1093/advances/nmx011
46. Ireson C, Orr S, Jones DJ, et al. Characterization of metabolites of the chemopreventive agent curcumin in human and rat hepatocytes and in the rat in vivo, and evaluation of their ability to inhibit phorbol ester-induced prostaglandin E2 production. *Cancer Res*. 2001;61(3):1058–1064.

47. Vareed SK, Kakarala M, Ruffin MT, et al. Pharmacokinetics of curcumin conjugate metabolites in healthy human subjects. *Cancer Epidemiol Biomarkers Prev*. 2008;17(6):1411–1417. doi:10.1158/1055-9965.Epi-07-2693
48. Cheng D, Li W, Wang L, et al. Pharmacokinetics, pharmacodynamics, and PKPD modeling of curcumin in regulating antioxidant and epigenetic gene expression in healthy human volunteers. *Mol Pharm*. 2019;16(5):1881–1889. doi:10.1021/acs.molpharmaceut.8b01246
49. Prasad S, Gupta SC, Tyagi AK, Aggarwal BB. Curcumin, a component of golden spice: from bedside to bench and back. *Biotechnol Adv*. 2014;32(6):1053–1064. doi:10.1016/j.biotechadv.2014.04.004
50. Anand P, Kunnumakkara AB, Newman RA, Aggarwal BB. Bioavailability of curcumin: problems and promises. *Mol Pharm*. 2007;4 (6):807–818. doi:10.1021/mp700113r
51. Kunnumakkara AB, Bordoloi D, Padmavathi G, et al. Curcumin, the golden nutraceutical: multitargeting for multiple chronic diseases. *Br J Pharmacol*. 2017;174(11):1325–1348. doi:10.1111/bph.13621
52. Ireson CR, Jones DJ, Orr S, et al. Metabolism of the cancer chemopreventive agent curcumin in human and rat intestine. *Cancer Epidemiol Biomarkers Prev*. 2002;11:105–111.
53. Asai A, Miyazawa T. Occurrence of orally administered curcuminoid as glucuronide and glucuronide/sulfate conjugates in rat plasma. *Life Sci*. 2000;67(23):2785–2793. doi:10.1016/s0024-3205(00)00868-7
54. Sørlie T, Perou CM, Tibshirani R, et al. Gene expression patterns of breast carcinomas distinguish tumor subclasses with clinical implications. *Proc Natl Acad Sci U S A*. 2001;98(19):10869–10874. doi:10.1073/pnas.191367098
55. Wheatley DN. A new journal – "theoretical biology and medical modelling". *Theor Biol Med Model*. 2005;2(1):21. doi:10.1186/1742-4682-2-21
56. Wang Y, Yu J, Cui R, Lin J, Ding X. Curcumin in treating breast cancer: a review. *J Lab Autom*. 2016;21:723–731. doi:10.1177/2211068216655524
57. Sethiya A, Agarwal DK, Agarwal S. Current trends in drug delivery system of curcumin and its therapeutic applications. *Mini Rev Med Chem*. 2020;20:1190–1232. doi:10.2174/1389557520666200429103647
58. Obeid MA, Alsaadi M, Aljabali AA. Recent updates in curcumin delivery. *J Liposome Res*. 2022;1–12. doi:10.1080/08982104.2022.2086567
59. Ströfer M, Jelkmann W, Depping R. Curcumin decreases survival of Hep3B liver and MCF-7 breast cancer cells: the role of HIF. *Strahlenther Onkol*. 2011;187:393–400. doi:10.1007/s00066-011-2248-0
60. Altenburg JD, Bieberich AA, Terry C, et al. A synergistic antiproliferation effect of curcumin and docosahexaenoic acid in SK-BR-3 breast cancer cells: unique signaling not explained by the effects of either compound alone. *BMC Cancer*. 2011;11(1):149. doi:10.1186/1471-2407-11-149
61. Shao Z-M, Shen -Z-Z, Liu C-H, et al. Curcumin exerts multiple suppressive effects on human breast carcinoma cells. *Int J Oncol*. 2002;98 (2):234–240. doi:10.1002/ijc.10183
62. Slamon DJ, Clark GM, Wong SG, et al. Human breast cancer: correlation of relapse and survival with amplification of the HER-2/ neu oncogene. *Science*. 1987;235(4785):177–182. doi:10.1126/science.3798106
63. Shishodia S, Chaturvedi MM, Aggarwal BB. Role of curcumin in cancer therapy. *Curr Probl Cancer*. 2007;31:243–305. doi:10.1016/j.currproblcancer.2007.04.001
64. Ke C-S, Liu H-S, Yen C-H, et al. Curcumin-induced aurora-a suppression not only causes mitotic defect and cell cycle arrest but also alters chemosensitivity to anticancer drugs. *J Nutr Biochem*. 2014;25(5):526–539. doi:10.1016/j.jnutbio.2014.01.003
65. Zhou Q-M, Wang X-F, Liu X-J, et al. Curcumin enhanced antiproliferative effect of mitomycin C in human breast cancer MCF-7 cells in vitro and in vivo. *Acta Pharmacol Sin*. 2011;32(11):1402–1410. doi:10.1038/aps.2011.97
66. Kim J-M, Noh E-M, Kwon K-B, et al. Curcumin suppresses the TPA-induced invasion through inhibition of PKCα-dependent MMP-expression in MCF-7 human breast cancer cells. *Phytomedicine*. 2012;19(12):1085–1092. doi:10.1016/j.phymed.2012.07.002
67. Hassan ZK, Daghestani MH. Curcumin effect on MMPs and TIMPs genes in a breast cancer cell line. *Asian Pac J Cancer Prev*. 2012;13 (7):3259–3264. doi:10.7314/apjcp.2012.13.7.3259
68. Bachmeier BE, Mohrenz IV, Mirisola V, et al. Curcumin downregulates the inflammatory cytokines CXCL1 and −2 in breast cancer cells via NFkappaB. *Carcinogenesis*. 2008;29(4):779–789. doi:10.1093/carcin/bgm248
69. Xia Y, Jin L, Zhang B, et al. The potentiation of curcumin on insulin-like growth factor-1 action in MCF-7 human breast carcinoma cells. *Life Sci*. 2007;80(23):2161–2169. doi:10.1016/j.lfs.2007.04.008
70. Narasimhan SR, Yang L, Gerwin BI, Broaddus VC. Resistance of pleural mesothelioma cell lines to apoptosis: relation to expression of Bcl-2 and Bax. *Am J Physiol*. 1998;275(1):L165–171. doi:10.1152/ajplung.1998.275.1.L165
71. Nagaraju GP, Zhu S, Ko JE, et al. Antiangiogenic effects of a novel synthetic curcumin analogue in pancreatic cancer. *Cancer Lett*. 2015;357 (2):557–565. doi:10.1016/j.canlet.2014.12.007
72. Abadi AJ, Mirzaei S, Mahabady MK, et al. Curcumin and its derivatives in cancer therapy: potentiating antitumor activity of cisplatin and reducing side effects. *Phytother Res*. 2022;36(1):189–213. doi:10.1002/ptr.7305
73. Bhattacharyya S, Md Sakib Hossain D, Mohanty S, et al. Curcumin reverses T cell-mediated adaptive immune dysfunctions in tumor-bearing hosts. *Cell Mol Immunol*. 2010;7(4):306–315. doi:10.1038/cmi.2010.11
74. Abbasalizadeh F, Alizadeh E, Bagher Fazljou SM, Torbati M, Akbarzadeh A. Anticancer effect of alginate-chitosan hydrogel loaded with curcumin and chrysin on lung and breast cancer cell lines. *Curr Drug Deliv*. 2022;19:600–613. doi:10.2174/1567201818666210813142007
75. Abbasi S, Kajimoto K, Harashima H. Critical parameters dictating efficiency of membrane-mediated drug transfer using nanoparticles. *Int J Pharm*. 2018;553(1–2):398–407. doi:10.1016/j.ijpharm.2018.10.042
76. Jafarinejad-Farsangi S, Hashemi MS, Yazdi Rouholamini SE, et al. Curcumin loaded on graphene nanosheets induced cell death in mammospheres from MCF-7 and primary breast tumor cells. *Biomed Mater*. 2021;16(4):045040. doi:10.1088/1748-605X/ac0400
77. Jahanshahi M, Kowsari E, Haddadi-Asl V, et al. Sericin grafted multifunctional curcumin loaded fluorinated graphene oxide nanomedicines with charge switching properties for effective cancer cell targeting. *Int J Pharm*. 2019;572:118791. doi:10.1016/j.ijpharm.2019.118791
78. Jaisamut P, Wiwattanawongsa K, Graidist P, Sangsen Y, Wiwattanapatapee R. Enhanced oral bioavailability of curcumin using a supersaturatable self-microemulsifying system incorporating a hydrophilic polymer; in vitro and in vivo investigations. *AAPS PharmSciTech*. 2018;19(2):730–740. doi:10.1208/s12249-017-0857-3
79. Jaiswal S, Mishra P. Co-delivery of curcumin and serratiopeptidase in HeLa and MCF-7 cells through nanoparticles show improved anti-cancer activity. *Mater Sci Eng C Mater Biol Appl*. 2018;92:673–684. doi:10.1016/j.msec.2018.07.025

80. Bao C, Jiang P, Chai J, et al. The delivery of sensitive food bioactive ingredients: absorption mechanisms, influencing factors, encapsulation techniques and evaluation models. *Food Res Int*. 2019;120:130–140. doi:10.1016/j.foodres.2019.02.024
81. Du M, Ouyang Y, Meng F, et al. Nanotargeted agents: an emerging therapeutic strategy for breast cancer. *Nanomedicine*. 2019;14 (13):1771–1786. doi:10.2217/nnm-2018-0481
82. Fraguas-Sánchez AI, Lozza I, Torres-Suárez AI. Actively targeted nanomedicines in breast cancer: from pre-clinal investigation to clinic. *Cancers*. 2022;14(5):1198. doi:10.3390/cancers14051198
83. Ganesan K, Wang Y, Gao F, et al. Targeting engineered nanoparticles for breast cancer therapy. *Pharmaceutics*. 2021;13(11):1829. doi:10.3390/pharmaceutics13111829
84. Alqaraghuli HGJ, Kashanian S, Rafipour R. A review on targeting nanoparticles for breast cancer. *Curr Pharm Biotechnol*. 2019;20 (13):1087–1107. doi:10.2174/1389201020666190731130001
85. Dong Z, Cui M-Y, Peng Z, et al. Nanoparticles for colorectal cancer targeted drug delivery and MR imaging: current situation and perspectives. *Curr Cancer Drug Targets*. 2016;16(6):536–550. doi:10.2174/1568009616666151130214442
86. Gary-Bobo M, Vaillant O, Maynadier M, et al. Targeting multiplicity: the key factor for anti-cancer nanoparticles. *Curr Med Chem*. 2013;20 (15):1946–1955. doi:10.2174/0929867311320150002
87. Grinberg S, Linder C, Heldman E. Progress in lipid-based nanoparticles for cancer therapy. *Crit Rev Oncog*. 2014;19(3–4):247–260. doi:10.1615/critrevoncog.2014011815
88. Sun T, Zhang YS, Pang B, et al. Engineered nanoparticles for drug delivery in cancer therapy. *Angew Chem*. 2014;53(46):12320–12364. doi:10.1002/anie.201403036
89. Hamano N, Böttger R, Lee SE, et al. Robust microfluidic technology and new lipid composition for fabrication of curcumin-loaded liposomes: effect on the anticancer activity and safety of cisplatin. *Mol Pharm*. 2019;16(9):3957–3967. doi:10.1021/acs.molpharmaceut.9b00583
90. Hasan M, Elkhoury K, Belhaj N, et al. Growth-inhibitory effect of chitosan-coated liposomes encapsulating curcumin on MCF-7 breast cancer cells. *Mar Drugs*. 2020;18(4):217. doi:10.3390/md18040217
91. Li R, Deng L, Cai Z, et al. Liposomes coated with thiolated chitosan as drug carriers of curcumin. *Mater Sci Eng C Mater Biol Appl*. 2017;80:156–164. doi:10.1016/j.msec.2017.05.136
92. Mahmoudi R, Hassandokht F, Ardakani MT, et al. Intercalation of curcumin into liposomal chemotherapeutic agent augments apoptosis in breast cancer cells. *J Biomater Appl*. 2021;35(8):1005–1018. doi:10.1177/0885328220976331
93. Karabasz A, Lachowicz D, Karewicz A, et al. Analysis of toxicity and anticancer activity of micelles of sodium alginate-curcumin. *Int J Nanomedicine*. 2019;14:7249–7262. doi:10.2147/ijn.S213942
94. Muddineti OS, Vanaparthi A, Rompicharla SVK, et al. Cholesterol and vitamin E-conjugated PEGylated polymeric micelles for efficient delivery and enhanced anticancer activity of curcumin: evaluation in 2D monolayers and 3D spheroids. *Artif Cells, Nanomed Biotechnol*. 2018;46(sup1):773–786. doi:10.1080/21691401.2018.1435551
95. Sarika PR, Nirmala RJ. Curcumin loaded gum Arabic aldehyde-gelatin nanogels for breast cancer therapy. *Mater Sci Eng C Mater Biol Appl*. 2016;65:331–337. doi:10.1016/j.msec.2016.04.044
96. Nguyen NT, Bui QA, Nguyen HHN, et al. Curcuminoid co-loading platinum heparin-poloxamer P403 Nanogel increasing effectiveness in antitumor activity. *Gels*. 2022;8(1):59. doi:10.3390/gels8010059
97. Wang W, Chen T, Xu H, et al. Curcumin-loaded solid lipid nanoparticles enhanced anticancer efficiency in breast cancer. *Molecules*. 2018;23. doi:10.3390/molecules23071578
98. Fathy Abd-Ellatef G-E, Gazzano E, Chirio D, et al. Curcumin-loaded solid lipid nanoparticles bypass P-glycoprotein mediated doxorubicin resistance in triple negative breast cancer cells. *Pharmaceutics*. 2020;12(2):96. doi:10.3390/pharmaceutics12020096
99. Meena R, Kumar S, Kumar R, Gaharwar US, Rajamani P. PLGA-CTAB curcumin nanoparticles: fabrication, characterization and molecular basis of anticancer activity in triple negative breast cancer cell lines (MDA-MB-231 cells). *Biomed Pharmacother*. 2017;94:944–954. doi:10.1016/j.biopha.2017.07.151
100. Vakilinezhad MA, Amini A, Dara T, Alipour S. Methotrexate and Curcumin co-encapsulated PLGA nanoparticles as a potential breast cancer therapeutic system: in vitro and in vivo evaluation. *Colloids Surf B Biointerfaces*. 2019;184:110515. doi:10.1016/j.colsurfb.2019.110515
101. Abdel-Hakeem MA, Mongy S, Hassan B, Tantawi OI, Badawy I. Curcumin loaded chitosan-protamine nanoparticles revealed antitumor activity via suppression of NF-κB, proinflammatory cytokines and Bcl-2 gene expression in the breast cancer cells. *J Pharm Sci*. 2021;110 (9):3298–3305. doi:10.1016/j.xphs.2021.06.004
102. Kamalabadi-Farahani M, Vasei M, Ahmadbeigi N, et al. Anti-tumour effects of TRAIL-expressing human placental derived mesenchymal stem cells with curcumin-loaded chitosan nanoparticles in a mice model of triple negative breast cancer. *Artif Cells Nanomed Biotechnol*. 2018;46 (sup3):S1011–s1021. doi:10.1080/21691401.2018.1527345
103. Lin J, Cai Q, Tang Y, et al. PEGylated lipid bilayer coated mesoporous silica nanoparticles for co-delivery of paclitaxel and curcumin: design, characterization and its cytotoxic effect. *Int J Pharm*. 2018;536(1):272–282. doi:10.1016/j.ijpharm.2017.10.043
104. Khandelwal P, Alam A, Choksi A, Chattopadhyay S, Poddar P. Retention of anticancer activity of curcumin after conjugation with fluorescent gold quantum clusters: an in vitro and in vivo xenograft study. *ACS omega*. 2018;3(5):4776–4785. doi:10.1021/acsomega.8b00113
105. Vemuri SK, Halder S, Banala RR, et al. Modulatory effects of biosynthesized gold nanoparticles conjugated with curcumin and paclitaxel on tumorigenesis and metastatic pathways-in vitro and in vivo studies. *Int J Mol Sci*. 2022;23(4):2150. doi:10.3390/ijms23042150
106. Bharmoria P, Bisht M, Gomes MC, et al. Protein-olive oil-in-water nanoemulsions as encapsulation materials for curcumin acting as anticancer agent towards MDA-MB-231 cells. *Sci Rep*. 2021;11(1):9099. doi:10.1038/s41598-021-88482-3
107. Kazi M, Nasr F, Noman O, et al. Development, characterization optimization, and assessment of curcumin-loaded bioactive self-nanoemulsifying formulations and their inhibitory effects on human breast cancer MCF-7 cells. *Pharmaceutics*. 2020;12(11):1107. doi:10.3390/pharmaceutics12111107
108. Aqil F, Munagala R, Jeyabalan J, Agrawal AK, Gupta R. Exosomes for the enhanced tissue bioavailability and efficacy of curcumin. *AAPS J*. 2017;19(6):1691–1702. doi:10.1208/s12248-017-0154-9
109. González-Sarrías A, Iglesias-Aguirre CE, Cortés-Martín A, et al. Milk-derived exosomes as nanocarriers to deliver curcumin and resveratrol in breast tissue and enhance their anticancer activity. *Int J Mol Sci*. 2022;23(5):2860. doi:10.3390/ijms23052860

110. Galisteo-González F, Molina-Bolívar JA, Navarro SA, et al. Albumin-covered lipid nanocapsules exhibit enhanced uptake performance by breast-tumor cells. *Colloids Surf B Biointerfaces*. 2018;165:103–110. doi:10.1016/j.colsurfb.2018.02.024
111. De D, Das CK, Mandal D, et al. Curcumin complexed with graphene derivative for breast cancer therapy. *ACS Appl Bio Mater*. 2020;3 (9):6284–6296. doi:10.1021/acsabm.0c00771
112. Malam Y, Loizidou M, Seifalian AM. Liposomes and nanoparticles: nanosized vehicles for drug delivery in cancer. *Trends Pharmacol Sci*. 2009;30(11):592–599. doi:10.1016/j.tips.2009.08.004
113. Chapman HD, Rathinam T. Focused review: the role of drug combinations for the control of coccidiosis in commercially reared chickens. *Int J Parasitol Drugs Drug Resist*. 2022;18:32–42. doi:10.1016/j.ijpddr.2022.01.001
114. Mancia G, Rea F, Corrao G, Grassi G. Two-drug combinations as first-step antihypertensive treatment. *Circ Res*. 2019;124(7):1113–1123. doi:10.1161/circresaha.118.313294
115. van Hasselt JGC, Iyengar R. Systems pharmacology: defining the interactions of drug combinations. *Annu Rev Pharmacol Toxicol*. 2019;59 (1):21–40. doi:10.1146/annurev-pharmtox-010818-021511
116. Walker AJ. Regulatory considerations in the development of radiation-drug combinations. *Int J Radiat Oncol Biol Phys*. 2021;111 (5):1140–1144. doi:10.1016/j.ijrobp.2021.07.1710
117. Wu Y-L, Li Z. The perspectives of using unimolecular micelles in nanodrug formulation. *Ther Deliv*. 2019;10(6):333–335. doi:10.4155/tde-2019-0033
118. Zhang L, Shi D, Shi C, Kaneko T, Chen M. Supramolecular micellar drug delivery system based on multi-arm block copolymer for highly effective encapsulation and sustained-release chemotherapy. *J Mater Chem B*. 2019;7(37):5677–5687. doi:10.1039/c9tb01221d
119. Wan Z, Zheng R, Moharil P, et al. Polymeric micelles in cancer immunotherapy. *Molecules*. 2021;26(5):1220. doi:10.3390/molecules26051220
120. Costa D, Santo D, Domingues C, et al. Recent advances in peptide-targeted micelleplexes: current developments and future perspectives. *Int J Pharm*. 2021;597:120362. doi:10.1016/j.ijpharm.2021.120362
121. Pereira P, Barreira M, Queiroz JA, et al. Smart micelleplexes as a new therapeutic approach for RNA delivery. *Expert Opin Drug Deliv*. 2017;14 (3):353–371. doi:10.1080/17425247.2016.1214567
122. Dong S, Jiang Y, Qin G, Liu L, Zhao H. Methionine-based pH and oxidation dual-responsive block copolymer: synthesis and fabrication of protein nanogels. *Biomacromolecules*. 2020;21(10):4063–4075. doi:10.1021/acs.biomac.0c00879
123. Wang H, Gao L, Fan T, et al. Strategic design of intelligent-responsive nanogel carriers for cancer therapy. *ACS Appl Mater Interfaces*. 2021;13 (46):54621–54647. doi:10.1021/acsami.1c13634
124. Ferreira Soares DC, Domingues SC, Viana DB, Tebaldi ML. Polymer-hybrid nanoparticles: current advances in biomedical applications. *Biomed Pharmacother*. 2020;131:110695. doi:10.1016/j.biopha.2020.110695
125. Nicolas J, Couvreur P. Les nanoparticules polymères pour la délivrance de principes actifs anticancéreux [Polymer nanoparticles for the delivery of anticancer drug]. *Med Sci*. 2017;33(1):11–17. French. doi:10.1051/medsci/20173301003
126. Grill AE, Shahani K, Koniar B, Panyam J. Chemopreventive efficacy of curcumin-loaded PLGA microparticles in a transgenic mouse model of HER-2-positive breast cancer. *Drug Deliv Transl Res*. 2018;8(2):329–341. doi:10.1007/s13346-017-0377-4
127. Sheikh A, Md S, Alhakamy NA, Kesharwani P. Recent development of aptamer conjugated chitosan nanoparticles as cancer therapeutics. *Int J Pharm*. 2022;620:121751. doi:10.1016/j.ijpharm.2022.121751
128. Ryu JH, Yoon HY, Sun IC, Kwon IC, Kim K. Tumor-targeting glycol chitosan nanoparticles for cancer heterogeneity. *Adv Mater*. 2020;32(51): e2002197. doi:10.1002/adma.202002197
129. Rizeq BR, Younes NN, Rasool K, Nasrallah GK. Synthesis, bioapplications, and toxicity evaluation of chitosan-based nanoparticles. *Int J Mol Sci*. 2019;20(22):5776. doi:10.3390/ijms20225776
130. Hurvitz S, Mead M. Triple-negative breast cancer: advancements in characterization and treatment approach. *Curr Opin Obstet Gynecol*. 2016;28:59–69. doi:10.1097/gco.0000000000000239
131. Wu GS. TRAIL as a target in anti-cancer therapy. *Cancer Lett*. 2009;285(1):1–5. doi:10.1016/j.canlet.2009.02.029
132. Chen C, Sun W, Wang X, Wang Y, Wang P. Rational design of curcumin loaded multifunctional mesoporous silica nanoparticles to enhance the cytotoxicity for targeted and controlled drug release. *Mater Sci Eng C Mater Biol Appl*. 2018;85:88–96. doi:10.1016/j.msec.2017.12.007
133. Shah S, Famta P, Bagasariya D, et al. Tuning mesoporous silica nanoparticles in novel avenues of cancer therapy. *Mol Pharm*. 2022;19 (12):4428–4452. doi:10.1021/acs.molpharmaceut.2c00374
134. Gao J, Fan K, Jin Y, et al. PEGylated lipid bilayer coated mesoporous silica nanoparticles co-delivery of paclitaxel and curcumin leads to increased tumor site drug accumulation and reduced tumor burden. *Eur J Pharm Sci*. 2019;140:105070. doi:10.1016/j.ejps.2019.105070
135. Danafar H, Sharafi A, Askarlou S, Manjili HK. Preparation and characterization of PEGylated iron oxide-gold nanoparticles for delivery of sulforaphane and curcumin. *Drug Res*. 2017;67(12):698–704. doi:10.1055/s-0043-115905
136. Danafar H, Sharafi A, Kheiri S, Kheiri Manjili H. Co -delivery of sulforaphane and curcumin with PEGylated iron oxide-gold core shell nanoparticles for delivery to breast cancer cell line. *Iran J Pharm Sci*. 2018;17:480–494.
137. Zhang B, Zhou X, Miao Y, et al. Effect of phosphatidylcholine on the stability and lipolysis of nanoemulsion drug delivery systems. *Int J Pharm*. 2020;583:119354. doi:10.1016/j.ijpharm.2020.119354
138. Sánchez-López E, Guerra M, Dias-Ferreira J, et al. Current applications of nanoemulsions in cancer therapeutics. *Nanomaterials*. 2019;9 (6):821. doi:10.3390/nano9060821
139. Ganta S, Talekar M, Singh A, Coleman TP, Amiji MM. Nanoemulsions in translational research-opportunities and challenges in targeted cancer therapy. *AAPS PharmSciTech*. 2014;15(3):694–708. doi:10.1208/s12249-014-0088-9
140. Srivastava S, Haider MF, Ahmad A, et al. Exploring nanoemulsions for prostate cancer therapy. *Drug Res*. 2021;71(08):417–428. doi:10.1055/a-1518-6606
141. Zhou L, Zou M, Xu Y, et al. Nano drug delivery system for tumor immunotherapy: next-generation therapeutics. *Front Oncol*. 2022;12:864301. doi:10.3389/fonc.2022.864301
142. Bazak R, Houri M, El Achy S, Kamel S, Refaat T. Cancer active targeting by nanoparticles: a comprehensive review of literature. *J Cancer Res Clin Oncol*. 2015;141(5):769–784. doi:10.1007/s00432-014-1767-3
143. Ashique S, Sandhu NK, Chawla V, Chawla PA. Targeted drug delivery: trends and perspectives. *Curr Drug Deliv*. 2021;18(10):1435–1455. doi:10.2174/1567201818666210609161301

144. He F, Wen N, Xiao D, et al. Aptamer-based targeted drug delivery systems: current potential and challenges. *Curr Med Chem*. 2020;27(13):2189–2219. doi:10.2174/0929867325666181008142831
145. Lin Y-L, Tsai N-M, Chen C-H, et al. Specific drug delivery efficiently induced human breast tumor regression using a lipoplex by non-covalent association with anti-tumor antibodies. *J Nanobiotechnology*. 2019;17(1):25. doi:10.1186/s12951-019-0457-3
146. Saleh T, Soudi T, Shojaosadati SA. Aptamer functionalized curcumin-loaded human serum albumin (HSA) nanoparticles for targeted delivery to HER-2 positive breast cancer cells. *Int J Biol Macromol*. 2019;130:109–116. doi:10.1016/j.ijbiomac.2019.02.129
147. Duan D, Wang A, Ni L, et al. Trastuzumab- and Fab′ fragment-modified curcumin PEG-PLGA nanoparticles: preparation and evaluation in vitro and in vivo. *Int J Nanomedicine*. 2018;13:1831–1840. doi:10.2147/ijn.S153795
148. Jin H, Pi J, Zhao Y, et al. EGFR-targeting PLGA-PEG nanoparticles as a curcumin delivery system for breast cancer therapy. *Nanoscale*. 2017;9(42):16365–16374. doi:10.1039/c7nr06898k
149. Ghosh S, Dutta S, Sarkar A, Kundu M, Sil PC. Targeted delivery of curcumin in breast cancer cells via hyaluronic acid modified mesoporous silica nanoparticle to enhance anticancer efficiency. *Colloids Surf B Biointerfaces*. 2021;197:111404. doi:10.1016/j.colsurfb.2020.111404
150. Soleymani M, Velashjerdi M, Asgari M. Preparation of hyaluronic acid-decorated mixed nanomicelles for targeted delivery of hydrophobic drugs to CD44-overexpressing cancer cells. *Int J Pharm*. 2021;592:120052. doi:10.1016/j.ijpharm.2020.120052
151. Sun Y, Li X, Zhang L, et al. Cell permeable NBD peptide-modified liposomes by hyaluronic acid coating for the synergistic targeted therapy of metastatic inflammatory breast cancer. *Mol Pharm*. 2019;16(3):1140–1155. doi:10.1021/acs.molpharmaceut.8b01123
152. Zhao Y, Wang K, Zheng Y, et al. Co-delivery of salinomycin and curcumin for cancer stem cell treatment by inhibition of cell proliferation, cell cycle arrest, and epithelial-mesenchymal transition. *Front Chem*. 2021;8:601649. doi:10.3389/fchem.2020.601649
153. Mahmoudi R, Ashraf Mirahmadi-Babaheidri S, Delaviz H, et al. RGD peptide-mediated liposomal curcumin targeted delivery to breast cancer cells. *J Biomater Appl*. 2021;35(7):743–753. doi:10.1177/0885328220949367
154. Hasanpoor Z, Mostafaie A, Nikokar I, Hassan ZM. Curcumin-human serum albumin nanoparticles decorated with PDL1 binding peptide for targeting PDL1-expressing breast cancer cells. *Int J Biol Macromol*. 2020;159:137–153. doi:10.1016/j.ijbiomac.2020.04.130
155. Lin M, Teng L, Wang Y, Zhang J, Sun X. Curcumin-guided nanotherapy: a lipid-based nanomedicine for targeted drug delivery in breast cancer therapy. *Drug Deliv*. 2016;23:1420–1425. doi:10.3109/10717544.2015.1066902
156. Esfandiarpour-Boroujeni S, Bagheri-Khoulenjani S, Mirzadeh H, Amanpour S. Fabrication and study of curcumin loaded nanoparticles based on folate-chitosan for breast cancer therapy application. *Carbohydr Polym*. 2017;168:14–21. doi:10.1016/j.carbpol.2017.03.031
157. Pal K, Laha D, Parida PK, et al. An in vivo study for targeted delivery of curcumin in human triple negative breast carcinoma cells using biocompatible PLGA microspheres conjugated with folic acid. *J Nanosci Nanotechnol*. 2019;19:3720–3733. doi:10.1166/jnn.2019.16292
158. Cui T, Zhang S, Sun H. Co-delivery of doxorubicin and pH-sensitive curcumin prodrug by transferrin-targeted nanoparticles for breast cancer treatment. *Oncol Rep*. 2017;37(2):1253–1260. doi:10.3892/or.2017.5345
159. Nahta R, Yu D, Hung M-C, Hortobagyi GN, Esteva FJ. Mechanisms of disease: understanding resistance to HER2-targeted therapy in human breast cancer. *Nat Clin Pract Oncol*. 2006;3(5):269–280. doi:10.1038/ncponc0509
160. Wartlick H, Michaelis K, Balthasar S, et al. Highly specific HER2-mediated cellular uptake of antibody-modified nanoparticles in tumour cells. *J Drug Target*. 2004;12(7):461–471. doi:10.1080/10611860400010697
161. Steinhauser I, Spänkuch B, Strebhardt K, Langer K. Trastuzumab-modified nanoparticles: optimisation of preparation and uptake in cancer cells. *Biomaterials*. 2006;27(28):4975–4983. doi:10.1016/j.biomaterials.2006.05.016
162. Park JW, Hong K, Kirpotin DB, et al. Anti-HER2 immunoliposomes: enhanced efficacy attributable to targeted delivery. *Clin Cancer Res*. 2002;8:1172–1181.
163. Harrison PT, Vyse S, Huang PH. Rare epidermal growth factor receptor (EGFR) mutations in non-small cell lung cancer. *Semin Cancer Biol*. 2020;61:167–179. doi:10.1016/j.semcancer.2019.09.015
164. Sabbah DA, Hajjo R, Sweidan K. Review on Epidermal Growth Factor Receptor (EGFR) structure, signaling pathways, interactions, and recent updates of EGFR inhibitors. *Curr Top Med Chem*. 2020;20(10):815–834. doi:10.2174/1568026620666200303123102
165. Sigismund S, Avanzato D, Lanzetti L. Emerging functions of the EGFR in cancer. *Mol Oncol*. 2018;12:3–20. doi:10.1002/1878-0261.12155
166. Singh D, Attri BK, Gill RK, Bariwal J. Review on EGFR inhibitors: critical updates. *Mini Rev Med Chem*. 2016;16:1134–1166. doi:10.2174/1389557516666160321114917
167. Chen C, Zhao S, Karnad A, Freeman JW. The biology and role of CD44 in cancer progression: therapeutic implications. *J Hematol Oncol*. 2018;11(1):64. doi:10.1186/s13045-018-0605-5
168. Hassn Mesrati M, Syafruddin SE, Mohtar MA, Syahir A. CD44: a multifunctional mediator of cancer progression. *Biomolecules*. 2021;11(12):1850. doi:10.3390/biom11121850
169. Mattheolabakis G, Milane L, Singh A, Amiji MM. Hyaluronic acid targeting of CD44 for cancer therapy: from receptor biology to nanomedicine. *J Drug Target*. 2015;23(7–8):605–618. doi:10.3109/1061186x.2015.1052072
170. Shan D, Li J, Cai P, et al. RGD-conjugated solid lipid nanoparticles inhibit adhesion and invasion of αvβ3 integrin-overexpressing breast cancer cells. *Drug Deliv Transl Res*. 2015;5:15–26. doi:10.1007/s13346-014-0210-2
171. Wu PH, Onodera Y, Ichikawa Y, et al. Targeting integrins with RGD-conjugated gold nanoparticles in radiotherapy decreases the invasive activity of breast cancer cells. *Int J Nanomedicine*. 2017;85:5069–5085. doi:10.1016/j.msec.2017.12.007
172. Brooks PC, Clark RA, Cheresh DA. Requirement of vascular integrin alpha v beta 3 for angiogenesis. *Science*. 1994;264:569–571. doi:10.1126/science.7512751
173. Alipour M, Baneshi M, Hosseinkhani S, et al. Recent progress in biomedical applications of RGD-based ligand: from precise cancer theranostics to biomaterial engineering: a systematic review. *J Biomed Mater Res A*. 2020;108(4):839–850. doi:10.1002/jbm.a.36862
174. Cheng T-M, Chang W-J, Chu H-Y, et al. Nano-strategies targeting the integrin αvβ3 network for cancer therapy. *Cells*. 2021;10(7):1684. doi:10.3390/cells10071684
175. Luo J, Yao J-F, Deng X-F, et al. 14, 15-EET induces breast cancer cell EMT and cisplatin resistance by up-regulating integrin αvβ3 and activating FAK/PI3K/AKT signaling. *J Exp Clin Cancer Res*. 2018;37(1):23. doi:10.1186/s13046-018-0694-6
176. Gato-Cañas M, Zuazo M, Arasanz H, et al. PDL1 signals through conserved sequence motifs to overcome interferon-mediated cytotoxicity. *Cell Rep*. 2017;20(8):1818–1829. doi:10.1016/j.celrep.2017.07.075

177. Mittendorf EA, Philips AV, Meric-Bernstam F, et al. PD-L1 expression in triple-negative breast cancer. *Cancer Immunol Res*. 2014;2:361–370. doi:10.1158/2326-6066.Cir-13-0127
178. Kornepati AVR, Vadlamudi RK, Curiel TJ. Programmed death ligand 1 signals in cancer cells. *Nat Rev Cancer*. 2022;22:174–189. doi:10.1038/s41568-021-00431-4
179. Lei Q, Wang D, Sun K, Wang L, Zhang Y. Resistance mechanisms of anti-PD1/PDL1 therapy in solid tumors. *Front Cell Dev Biol*. 2020;8:672. doi:10.3389/fcell.2020.00672
180. Tran-Nguyen VK, Simeon S, Junaid M, Ballester PJ. Structure-based virtual screening for PDL1 dimerizers: evaluating generic scoring functions. *Curr Res Struct Biol*. 2022;4:206–210. doi:10.1016/j.crstbi.2022.06.002
181. Mi X, Hu M, Dong M, et al. Folic acid decorated zeolitic imidazolate framework (ZIF-8) loaded with baicalin as a nano-drug delivery system for breast cancer therapy. *Int J Nanomedicine*. 2021;16:8337–8352. doi:10.2147/ijn.S340764
182. Moazzen S, Dolatkhah R, Tabrizi JS, et al. Folic acid intake and folate status and colorectal cancer risk: a systematic review and meta-analysis. *Clin Nutr*. 2018;37:1926–1934. doi:10.1016/j.clnu.2017.10.010
183. Qin X, Cui Y, Shen L, et al. Folic acid supplementation and cancer risk: a meta-analysis of randomized controlled trials. *Int J Oncol*. 2013;133(5):1033–1041. doi:10.1002/ijc.28038
184. Qian ZM, Tang PL. Mechanisms of iron uptake by mammalian cells. *Biochim Biophys Acta*. 1995;1269:205–214. doi:10.1016/0167-4889(95)00098-x
185. Byrne JD, Betancourt T, Brannon-Peppas L. Active targeting schemes for nanoparticle systems in cancer therapeutics. *Adv Drug Deliv Rev*. 2008;60(15):1615–1626. doi:10.1016/j.addr.2008.08.005
186. Jefferies WA, Brandon MR, Hunt SV, et al. Transferrin receptor on endothelium of brain capillaries. *Nature*. 1984;312(5990):162–163. doi:10.1038/312162a0
187. Rosenblum D, Joshi N, Tao W, Karp JM, Peer D. Progress and challenges towards targeted delivery of cancer therapeutics. *Nat Commun*. 2018;9(1):1410. doi:10.1038/s41467-018-03705-y
188. Uthaman S, Huh KM, Park I-K. Tumor microenvironment-responsive nanoparticles for cancer theragnostic applications. *Biomater Res*. 2018;22(1):22. doi:10.1186/s40824-018-0132-z
189. Rashidzadeh H, Rezaei SJT, Zamani S, Sarijloo E, Ramazani A. pH-sensitive curcumin conjugated micelles for tumor triggered drug delivery. *J Biomater Sci Polym Ed*. 2021;32(3):320–336. doi:10.1080/09205063.2020.1833815
190. Ji P, Wang X, Yin J, et al. Selective delivery of curcumin to breast cancer cells by self-targeting apoferritin nanocages with pH-responsive and low toxicity. *Drug Deliv*. 2022;29(1):986–996. doi:10.1080/10717544.2022.2056662
191. Ghaffari SB, Sarrafzadeh MH, Salami M, Khorramizadeh MR. A pH-sensitive delivery system based on N-succinyl chitosan-ZnO nanoparticles for improving antibacterial and anticancer activities of curcumin. *Int J Biol Macromol*. 2020;151:428–440. doi:10.1016/j.ijbiomac.2020.02.141
192. Rejinold NS, Thomas RG, Muthiah M, et al. Breast tumor targetable Fe_3O_4 embedded thermo-responsive nanoparticles for radiofrequency assisted drug delivery. *J Biomed Nanotechnol*. 2016;12(1):43–55. doi:10.1166/jbn.2016.2135
193. Kulkarni AS, Tapase SR, Kodam KM, Shinde VS. Thermoresponsive pluronic based microgels for controlled release of curcumin against breast cancer cell line. *Colloids Surf B Biointerfaces*. 2021;205:111834. doi:10.1016/j.colsurfb.2021.111834
194. Howaili F, Özliseli E, Küçüktürkmen B, et al. Stimuli-responsive, plasmonic nanogel for dual delivery of curcumin and photothermal therapy for cancer treatment. *Front Chem*. 2021;8:602941. doi:10.3389/fchem.2020.602941
195. Sun M, Zhang Y, He Y, et al. Green synthesis of carrier-free curcumin nanodrugs for light-activated breast cancer photodynamic therapy. *Colloids Surf B Biointerfaces*. 2019;180:313–318. doi:10.1016/j.colsurfb.2019.04.061
196. Khorsandi K, Hosseinzadeh R, Shahidi FK. Photodynamic treatment with anionic nanoclays containing curcumin on human triple-negative breast cancer cells: cellular and biochemical studies. *J Cell Biochem*. 2019;120(4):4998–5009. doi:10.1002/jcb.27775
197. Nosrati H, Salehiabar M, Kheiri Manjili H, Davaran S, Danafar H. Theranostic nanoparticles based on magnetic nanoparticles: design, preparation, characterization, and evaluation as novel anticancer drug carrier and MRI contrast agent. *Drug Dev Ind Pharm*. 2018;44(10):1668–1678. doi:10.1080/03639045.2018.1483398
198. Jamshidifar E, Eshrati Yeganeh F, Shayan M, et al. Super magnetic niosomal nanocarrier as a new approach for treatment of breast cancer: a case study on SK-BR-3 and MDA-MB-231 cell lines. *Int J Mol Sci*. 2021;22(15):7948. doi:10.3390/ijms22157948
199. Mura S, Nicolas J, Couvreur P. Stimuli-responsive nanocarriers for drug delivery. *Nat Mater*. 2013;12(11):991–1003. doi:10.1038/nmat3776
200. Li Z, Huang J, Wu J. pH-sensitive nanogels for drug delivery in cancer therapy. *Biomater Sci*. 2021;9(3):574–589. doi:10.1039/d0bm01729a
201. Xiong MH, Bao Y, Yang X-Z, et al. Lipase-sensitive polymeric triple-layered nanogel for "on-demand" drug delivery. *J Am Chem Soc*. 2012;134(9):4355–4362. doi:10.1021/ja211279u
202. Bordat A, Boissenot T, Nicolas J, Tsapis N. Thermoresponsive polymer nanocarriers for biomedical applications. *Adv Drug Deliv Rev*. 2019;138:167–192. doi:10.1016/j.addr.2018.10.005
203. Zhou Y, Chen R, Yang H, et al. Light-responsive polymersomes with a charge-switch for targeted drug delivery. *J Mater Chem B*. 2020;8(4):727–735. doi:10.1039/c9tb02411e
204. Chen H, Ma Y, Wang X, Zha Z. Multifunctional phase-change hollow mesoporous Prussian blue nanoparticles as a NIR light responsive drug co-delivery system to overcome cancer therapeutic resistance. *J Mater Chem B*. 2017;5(34):7051–7058. doi:10.1039/c7tb01712j
205. Kamel AE, Fadel M, Louis D. Curcumin-loaded nanostructured lipid carriers prepared using Peceol™ and olive oil in photodynamic therapy: development and application in breast cancer cell line. *Int J Nanomedicine*. 2019;14:5073–5085. doi:10.2147/ijn.S210484
206. Li X, Li W, Wang M, Liao Z. Magnetic nanoparticles for cancer theranostics: advances and prospects. *J Control Release*. 2021;335:437–448. doi:10.1016/j.jconrel.2021.05.042
207. Liang Y, Duan L, Lu J, Xia J. Engineering exosomes for targeted drug delivery. *Theranostics*. 2021;11(7):3183–3195. doi:10.7150/thno.52570
208. Kalluri R, LeBleu VS. The biology, function, and biomedical applications of exosomes. *Science*. 2020;367. doi:10.1126/science.aau6977
209. Batrakova EV, Kim MS. Using exosomes, naturally-equipped nanocarriers, for drug delivery. *J Control Release*. 2015;219:396–405. doi:10.1016/j.jconrel.2015.07.030
210. Thanki K, Gangwal RP, Sangamwar AT, Jain S. Oral delivery of anticancer drugs: challenges and opportunities. *J Control Release*. 2013;170:15–40. doi:10.1016/j.jconrel.2013.04.020

211. Mora-Huertas CE, Fessi H, Elaissari A. Polymer-based nanocapsules for drug delivery. *Int J Pharm*. 2010;385(1–2):113–142. doi:10.1016/j.ijpharm.2009.10.018
212. Ansari MO, Gauthaman K, Essa A, Bencherif SA, Memic A. Graphene and graphene-based materials in biomedical applications. *Curr Med Chem*. 2019;26(38):6834–6850. doi:10.2174/0929867326666190705155854
213. Krishna KV, Ménard-Moyon C, Verma S, Bianco A. Graphene-based nanomaterials for nanobiotechnology and biomedical applications. *Nanomedicine*. 2013;8(10):1669–1688. doi:10.2217/nnm.13.140
214. Mukherjee SP, Bottini M, Fadeel B. Graphene and the immune system: a romance of many dimensions. *Front Immunol*. 2017;8:673. doi:10.3389/fimmu.2017.00673
215. Mirzaie Z, Reisi-Vanani A, Barati M, Atyabi SM. The drug release kinetics and anticancer activity of the GO/PVA-curcumin nanostructures: the effects of the preparation method and the GO amount. *J Pharm Sci*. 2021;110(11):3715–3725. doi:10.1016/j.xphs.2021.07.016
216. Sharma RA, Euden SA, Platton SL, et al. Phase I clinical trial of oral curcumin: biomarkers of systemic activity and compliance. *Clin Cancer Res*. 2004;10(20):6847–6854. doi:10.1158/1078-0432.Ccr-04-0744
217. Cruz–Correa M, Shoskes DA, Sanchez P, et al. Combination treatment with curcumin and quercetin of adenomas in familial adenomatous polyposis. *Clin Gastroenterol Hepatol*. 2006;4(8):1035–1038. doi:10.1016/j.cgh.2006.03.020
218. Howells LM, Iwuji COO, Irving GRB, et al. Curcumin combined with FOLFOX chemotherapy is safe and tolerable in patients with metastatic colorectal cancer in a randomized phase iia trial. *J Nutr*. 2019;149(7):1133–1139. doi:10.1093/jn/nxz029
219. Pricci M, Girardi B, Giorgio F, et al. Curcumin and colorectal cancer: from basic to clinical evidences. *Int J Mol Sci*. 2020;21(7):2364. doi:10.3390/ijms21072364
220. Termini D, Den Hartogh DJ, Jaglanian A, Tsiani E. Curcumin against prostate cancer: current evidence. *Biomolecules*. 2020;10(11):1536. doi:10.3390/biom10111536
221. Mortezaee K, Salehi E, Mirtavoos-mahyari H, et al. Mechanisms of apoptosis modulation by curcumin: implications for cancer therapy. *J Cell Physiol*. 2019;234(8):12537–12550. doi:10.1002/jcp.28122
222. Hassanalilou T, Ghavamzadeh S, Khalili L. Curcumin and gastric cancer: a review on mechanisms of action. *J Gastrointest Cancer*. 2019;50(2):185–192. doi:10.1007/s12029-018-00186-6
223. Wang L, Wang C, Tao Z, et al. Curcumin derivative WZ35 inhibits tumor cell growth via ROS-YAP-JNK signaling pathway in breast cancer. *J Exp Clin Cancer Res*. 2019;38(1):460. doi:10.1186/s13046-019-1424-4
224. Yin Y, Tan Y, Wei X, et al. Recent advances of curcumin derivatives in breast cancer. *Chem Biodivers*. 2022;19(10):e202200485. doi:10.1002/cbdv.202200485
225. Wang S, Chen Y, Guo J, Huang Q. Liposomes for tumor targeted therapy: a review. *Int J Mol Sci*. 2023;24. doi:10.3390/ijms24032643
226. De Leo V, Maurelli AM, Giotta L, Catucci L. Liposomes containing nanoparticles: preparation and applications. *Colloids Surf B Biointerfaces*. 2022;218:112737. doi:10.1016/j.colsurfb.2022.112737
227. Forouhari S, Beygi Z, Mansoori Z, et al. Liposomes: ideal drug delivery systems in breast cancer. *Biotechnol Appl Biochem*. 2022;69(5):1867–1884. doi:10.1002/bab.2253
228. Pandian SRK, Vijayakumar KK, Murugesan S, Kunjiappan S. Liposomes: an emerging carrier for targeting Alzheimer's and Parkinson's diseases. *Heliyon*. 2022;8:e09575. doi:10.1016/j.heliyon.2022.e09575
229. Tang C, McInnes BT. Cascade processes with micellar reaction media: recent advances and future directions. *Molecules*. 2022;27(17):5611. doi:10.3390/molecules27175611
230. Kaur J, Gulati M, Corrie L, et al. Role of nucleic acid-based polymeric micelles in treating lung diseases. *Nanomedicine*. 2022;17(25):1951–1960. doi:10.2217/nnm-2022-0260
231. Almajidi YQ, Kadhim MM, Alsaikhan F, et al. Doxorubicin-loaded micelles in tumor cell-specific chemotherapy. *Environ Res*. 2023;227:115722. doi:10.1016/j.envres.2023.115722
232. Yin Y, Hu B, Yuan X, et al. Nanogel: a versatile nano-delivery system for biomedical applications. *Pharmaceutics*. 2020;12(3):290. doi:10.3390/pharmaceutics12030290
233. Muraoka D, Harada N, Shiku H, Akiyoshi K. Self-assembled polysaccharide nanogel delivery system for overcoming tumor immune resistance. *J Control Release*. 2022;347:175–182. doi:10.1016/j.jconrel.2022.05.004
234. Zielińska A, Carreiró F, Oliveira AM, et al. Polymeric nanoparticles: production, characterization, toxicology and ecotoxicology. *Molecules*. 2020;25(16):3731. doi:10.3390/molecules25163731
235. Liu Y, Yang G, Jin S, Xu L, Zhao C-X. Development of high-drug-loading nanoparticles. *ChemPlusChem*. 2020;85(9):2143–2157. doi:10.1002/cplu.202000496
236. Pandey P, Gulati N, Makhija M, Purohit D, Dureja H. Nanoemulsion: a novel drug delivery approach for enhancement of bioavailability. *Recent Pat Nanotechnol*. 2020;14(4):276–293. doi:10.2174/1872210514666200604145755
237. Sabjan KB, Munawar SM, Rajendiran D, Vinoji SK, Kasinathan K. Nanoemulsion as oral drug delivery - a review. *Curr Drug Res Rev*. 2020;12(1):4–15. doi:10.2174/2589977511666191024173508
238. Zhao Z, Ukidve A, Kim J, Mitragotri S. Targeting strategies for tissue-specific drug delivery. *Cell*. 2020;181(1):151–167. doi:10.1016/j.cell.2020.02.001
239. Adepu S, Ramakrishna S. Controlled drug delivery systems: current status and future directions. *Molecules*. 2021;26(19):5905. doi:10.3390/molecules26195905
240. Patra JK, Das G, Fraceto LF, et al. Nano based drug delivery systems: recent developments and future prospects. *J Nanobiotechnol*. 2018;16(1):71. doi:10.1186/s12951-018-0392-8
241. Martín Giménez VM, Arya G, Zucchi IA, Galante MJ, Manucha W. Photo-responsive polymeric nanocarriers for target-specific and controlled drug delivery. *Soft Matter*. 2021;17(38):8577–8584. doi:10.1039/d1sm00999k
242. Heng PWS. Controlled release drug delivery systems. *Pharm Dev Technol*. 2018;23(9):833. doi:10.1080/10837450.2018.1534376